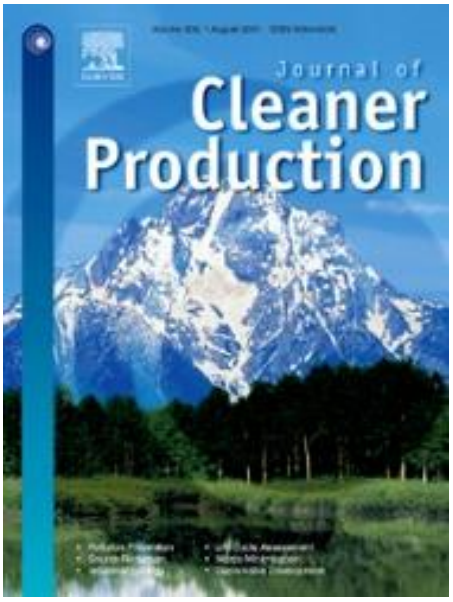

Journal of Cleaner Production

A Climate-based Analysis of Photosynthetically Active Radiation Availability in Large-Scale Greenhouses across China

Cong Wang[1,2], Jiangtao Du[3,*], Yu Liu[4], David Chow[3]

1) College of Urban Construction and Safety Engineering, Shanghai Institute of Technology, 201418, Shanghai, China

2) Department of Civil and Architectural Engineering, KTH Royal Institute of Technology, Brinellvägen 23, 100 44, Stockholm, Sweden

3) School of Architecture, University of Liverpool, Liverpool, L69 7ZN, UK

4) Sustainable Building and Environmental Research Institute, Northwestern Polytechnical University, 710072, Xi'an, China

Correspondence:

* Dr Jiangtao Du; Address: School of Architecture, University of Liverpool, Leverhulme Building, Abercromby Square, Liverpool, UK. Contact: jiangtao.du@liverpool.ac.uk

Abstract

Photosynthetically Active Radiation (PAR) is critically required for sustaining plant and vegetable growth. This study investigated PAR availabilities in two typical large-scale greenhouses using an advanced method of climate-based solar modelling in China. Seven Chinese locations in terms of daylight (solar) climate zones and latitudes were studied. The PAR prediction was conducted via RADIANCE (ray-tracing solar and light simulation package). Key findings are: 1) A climate-based analysis has been proved as more practical than the methods based on only clear sky and solar geometries. 2) A ray-tracing solar modelling can effectively predict PAR levels at specific positions (e.g. vertical planes), which would benefit the development of vertical farming activities. 3) The PAR availability would receive insignificant impact from roof configuration in these large-scale greenhouses. 4) For the approach of vertical farming, the vertical arrangement of planting system would be significantly affected by greenhouse orientations, while horizontally no such effect can be found. These findings could be developed into design strategies to support greenhouse planning.

Keywords

Photosynthetically Active Radiation (PAR), Greenhouse, RADIANCE simulation, Daylight climate zone, China

1. Introduction

With a rapidly increasing population, the food demand has been dramatically growing worldwide. The climate change and environment degradation such as dissertation and salinization of lands have further aggravated the food shortage (Panwar et al., 2011). The conventional open-field farming is confronted with challenges of uncertain climates and the stable food production suffers from inclement weather conditions (Ghoulem et al., 2019). Recently, the protected cultivation has been recognized as an effective solution to mitigate and adapt to climate change in food farming industries, especially in developing countries (Iddio et al., 2020). The greenhouse, one of the most important approaches of protected cultivation, was broadly applied using a lightweight structure covered by transparent medium to utilise the solar radiation. A greenhouse can protect plants from harsh external environments and provide an appropriate environment for the intensive production of various crops (Choab et al., 2019; Iddio et al., 2020).

1.1 Environmental factors in greenhouses

In greenhouses, critical environment factors affecting plant growth include light (Cossu et al., 2014), air temperature (Attar et al., 2014), humidity (Campen et al., 2003), CO_2 concentration (Ioslovich et al., 1995), and air movement (Cooper and Fuller, 1983).

Plants need light throughout their life cycle from germination and growth to flowering and seed production (Singh et al., 2015). The solar radiation (sunlight) provides the primary source of light for plants. However, plants do not absorb all wavelengths of solar radiation. The solar radiation in the spectrum range 400-700 nm, known as

photosynthetically active radiation (PAR), is responsible for the photosynthesis process, which is fundamental for the plant growth (Ciolkosz, 2008; Iddio et al., 2020). In the area of indoor farming, the PAR availability has been broadly applied as an indicator to justify the basic condition to keep a normal growing for plants in greenhouses (Kläring et al., 2012; Singh et al., 2015).

The air temperature influences most of the plant processes (Benni et al., 2016). The optimal temperature for the growth of most plants in greenhouses ranges between 17°C and 27°C, with extremes of 10°C and 35°C (Benni et al., 2016). Thus, greenhouses will be heated or cooled to maintain a suitable level of indoor air temperature based on the response to varying outdoor climates (Ahamed et al., 2019; Choab et al., 2019).

The humidity is also one of key factors in terms of the greenhouse indoor climate (Mortensen, 1986). The relative humidity (RH) inside greenhouses tends to be higher due to the transpiration of plants. High RH levels inside a greenhouse can not only slow down the plant's transpiration rate, but also induce a high risk of plants diseases and physiological disorders (Campen et al., 2003; Mortensen, 1986).

CO_2 is an essential raw ingredient required for the plant photosynthesis (Vox et al., 2010). However, the CO_2 levels within the greenhouse are usually low due to the CO_2 uptake by the plants. The CO_2 enrichment is found to be beneficial since it can increase the yield (Hao et al., 2020; Kläring et al., 2007; Kuroyanagi et al., 2014).

Maintaining proper airflow in greenhouses is of considerable importance for sustaining

the healthy growing of plants (Teitel et al., 2006). The recommended air speed inside a greenhouse is between 0.5 m/s and 0.7 m/s (Pakari and Ghani, 2019). Ventilation is one of the important factors determining the microclimate of a greenhouse (Fatnassi et al., 2004; Lee et al., 2018). Ventilation in summer is used to cool the greenhouse whilst ventilation can help remove excess moisture from the greenhouse in winter (Al-Helal et al., 2015; McCartney et al., 2018).

1.2 Environmental and energy performances in greenhouses

As an enclosed structure, a greenhouse allows the short wavelength solar radiation to enter through the transparent envelop and keeps the long wavelength solar radiation (Cao et al., 2019; Jain and Tiwari, 2002; Panwar et al., 2011). In order to maintain an optimal thermal environment for maximizing the plant growth rate, a large amount of energy will be needed to heat or cool the greenhouse using building service systems (Cao et al., 2019; Guo et al., 2020). The construction factors, such as materials, shapes, and orientations, as well as operational strategies, have a clear effect on the solar energy utilisation and thermal environment of a greenhouse (Ahamed et al., 2019; Ghoulem et al., 2019; Tong et al., 2013).

The cladding material is critical in determining the amount of solar radiation (including PAR) that enters the greenhouse (Pearson et al., 1995). Different materials of cladding (transparent or translucent) have different solar radiation transmittances. Some cladding materials that can control transmittance of sunlight in a specific range of wavelength have been recently applied in greenhouses to enhance PAR availability (Lamnatou and

Chemisana, 2013a, 2013b).

For the availability of solar radiation in a greenhouse, significant effects are found from its shapes and orientations (Ahamed et al., 2019; Kendirli, 2006). Gupta and Chandra (2002) studied the effect of different shapes, orientation and energy conservation measures on the heating requirements of greenhouses under cold climatic conditions of northern India. They found that the gothic arch shaped greenhouse required 2.6-4.2% less heating than the gable and quonset shapes and the east–west oriented gothic arch greenhouse required 2% less heating as compared to the north–south orientation. An investigation into the performance of five most used single-span shapes of greenhouses found that the uneven-span shape greenhouse received the highest level of solar radiation in each month of the year at all latitudes (Sethi, 2009). It was also noted that the east-west orientation was the most suited for year-round applications at all latitudes as this orientation received more radiation in winter and less in summer (Sethi, 2009). Similar findings were also presented by Chen et al. (2020), who concluded that the east-west orientation was the best in both winter and summer at all latitudes. As regards greenhouse shapes, they reported that the sawtooth-shaped greenhouse captured the highest amount of global solar radiation in winter at all latitudes. Çakır and Şahin (2015) compared five common greenhouse types and concluded that the elliptic type should be preferred for locations at the latitude of Bayburt. They also noted that, for a given type and floor area of greenhouses, the aspect ratio and orientation of the greenhouse should be optimized to best utilize the solar radiation. Another study of five typical shapes of greenhouse exposed

that the uneven span was the best solution in terms of minimising the energy consumption for maintaining the temperature favoured by plants (Singh and Tiwari, 2010). Similarly, using greenhouse models with various locations and orientations, El-Maghlany et al. (2015) supported that the east-west orientation can capture the maximum amount of solar heat gain. An Iranian investigation into six commonly used shapes of greenhouses has also found that the energy demand was the lowest in an east-west oriented single-span greenhouse with north brick wall (Mobtaker et al., 2019, 2016). Stanciu et al. (2016) compared the energy use of a greenhouse for vegetable farming in Romania under two orientations. The results indicated that the east-west orientation could consume less energy in both winter and summer compared with the north-south orientation, with an aim to maintain a stable indoor air temperature. Chen et al. (2018) proposed a modelling method to optimise the greenhouse orientation with respect to maximising solar energy collection and found that the optimal orientation was south by west (clock-wise rotation from east–west orientation), with the exact azimuth angle dependent on the latitude of the location. Using the 3D-shadow analysis in AutoCAD, Gupta et al. (2012) found that an orientation of 45° west of due south (southeast-northwest orientation) yielded maximum solar radiation collection in winter and minimum solar radiation collection in summer for the greenhouse in New Delhi (28.5°N). Table 1 provided an overview of the existing studies regarding the selection of greenhouse shape and orientation.

Ventilation is necessarily applied to achieve the optimal microclimate inside a greenhouse. Li et al. (2017) conducted detailed field measurement in two single-sloped Chinese

greenhouses and pointed out that the natural ventilation was a highly effective cooling solution in such greenhouses. Combining natural ventilation with evaporative cooling can significantly lower the greenhouse energy demand and provide crops with favourable growth conditions (Ghoulem et al., 2019). As greenhouse cooling is crucial for providing suitable growth conditions in hot climates, some wind-driven techniques have been proposed to enhance the nature ventilation. For instance, a passive downdraught evaporative cooling windcatcher (PDEC-WC) has been applied to greenhouses to enhance the greenhouse cooling and ventilation (Ghoulem et al., 2020a). The windcatcher ventilation is found to be able to provide higher airflow rates than conventional cross-flow ventilation when the greenhouse is surrounded by other structures (Ghoulem et al., 2020b).

As the increasing energy consumption in greenhouses has become an obstacle to sustainable farming, many renewable and sustainable energy technologies have been applied in greenhouses to reduce the heating, cooling, ventilation and lighting demand (Mirzamohammadi et al., 2020; Taki and Yildizhan, 2018). Such technologies include PV/PVT systems (Gorjian et al., 2021), phase change material (PCM) for thermal storage (Benli and Durmuş, 2009; Kooli et al., 2015), geothermal energy combined with heat pumps (Bakirci et al., 2011; Benli, 2013; Noorollahi et al., 2016), compost heat from organic waste (Neugebauer et al., 2021) and LED lighting (Singh et al., 2015). Ntinas et al. (2017) concluded that the greenhouse production using renewable energy could lead to even smaller environmental impact than the open-filed production. Control strategies

also play an important role in maintaining a favorable climate inside the greenhouse and reducing the energy consumption by efficiently coordinating the heating/cooling, ventilation and shading systems (Zhang et al., 2020).

1.3 Research gap and the present study

As mentioned above, solar radiation transmittance of envelop could be the first construction factor which designers and engineers of greenhouse will have to consider at an early planning stage. This architectural property of greenhouse can take significant and direct effect on the photosynthesis process of plants and the energy consumption of the whole facility. The effect of greenhouse shape, orientation, and structure on the solar energy collection has been well analysed in aforementioned studies. However, these analyses were conducted from the perspective of maximising solar heat gains and the purpose of these studies were to improve the greenhouse energy performance (i.e., reducing the heating or cooling need). The PAR availability, which is crucial for the growth of crops, has been neglected in these studies. From methodological point of view, the methods predicting solar heat gains in previous studies were based on solar geometries and assumptions (or statistics) of sky conditions (e.g., clear sky). Such methods may not be able to give convincing results considering the large temporal and spatial variability of climatic conditions of different locations. This may partly explain the inconsistency regarding the optimal shape and orientation in the literature. Greenhouses at the same latitude can have completely different profiles of PAR availability due to the different local climates. Even for the same greenhouse, the PAR availability varies from hour to

hour, from day to day, and from month to month. The demand for the light and thermal environment exhibits dynamic characteristics at different growth stages for many types of crops. Therefore, dynamic predictions of PAR availability taking into account the complex and variable characteristics of climate are urgently needed for the optimization and control of the greenhouse light environment. In addition, the optimal arrangement of crops inside the greenhouse will depend largely on the horizontal and vertical distribution of PAR. However, previous studies focused only on the cumulative effect of overall solar radiation received in the whole interior (i.e., the amount of heat gains over a certain period). There is a clear lack of studies that have evaluated PAR availability at specific time and at specific positions, e.g. the horizontal surface of greenhouse floor for growing low-height vegetation and the vertical surface of plant growing shelf (Wang et al., 2019). Recently, the 'Vertical Farming' (Kozai et al., 2016) has been developed in greenhouses as an efficient solution to increase food productions in a limited space, especially for such a facility located in urban areas (Sanjuan-Delmás et al., 2018). Thus, prediction and evaluation of PAR availability for vertical and horizontal planes at various heights will be necessarily required to meet the increasing activities of vertical farming in greenhouses.

China has a vast territory and the tremendous differences in latitude, longitude and altitude has made the climate of China extremely diverse. Based on the annual averaged daylight availability, China is divided into five daylight climate zones. In this article, a cross-region study of greenhouse performances in China was presented in terms of five daylight climate zones and seven locations. The availability of PAR in two typical large-

scale greenhouses was calculated at various horizontal and vertical planes using RADIANCE ("RADIANCE," 2020), which is an advanced ray-tracing package for solar (lighting) simulation in a complex environment. With the ray-tracing light simulation method, the PAR levels can be accurately predicted on an hourly basis over a period of an entire year at any position inside a greenhouse. The ray-tracing light simulation model was applied for the first time to analyse and compare the PAR levels in greenhouses of various shapes and orientations. It was also the first time a comprehensive climate-based analysis was implemented in order to produce design strategies for supporting greenhouse planning and construction across China.

2. Research methods and materials

2.1 Daylight climate zones and locations

As shown in Figure 1, in China, five daylight climate zones to indicate daylight (solar) availabilities in the built environment were recommended in one building regulation (Ministry of Housing and Urban-Rural Development, 2013). These five climate zones were defined according to the annual profile of solar irradiation monitored by 14 land-based weather stations across the country (Ministry of Housing and Urban-Rural Development, 2013). Table 2 presents the ranges of annual-averaged unobstructed illuminance (Eq) (produced from the monitored solar irradiation) at each zone. Seven big cities across China (Figure 1 & Table 2) have been selected as typical locations in this study, such as Lhasa (Zone I; 29.7°N, 91.1°E), Yinchuan (Zone II; 38.5°N, 106.2°E), Beijing (Zone III; 39.9°N, 116.4°E), Guangzhou (Zone IV; 23.1°N, 113.3°E), Wuhan

(Zone IV; 30.6°N, 114.3°E), Changchun (Zone IV; 43.8°N, 125.3°E), and Chengdu (Zone V; 30.6°N, 104.1°E). The highest and lowest annual solar irradiation levels are found at Lhasa and Chengdu respectively, while other locations have the levels in between. Selection of these locations was based on an aim to cover most of important agricultural regions in China. In order to simulate the PAR availability under real climate conditions, we adopted hourly weather data of the seven locations. The weather data were obtained via this source (https://energyplus.net/weather).

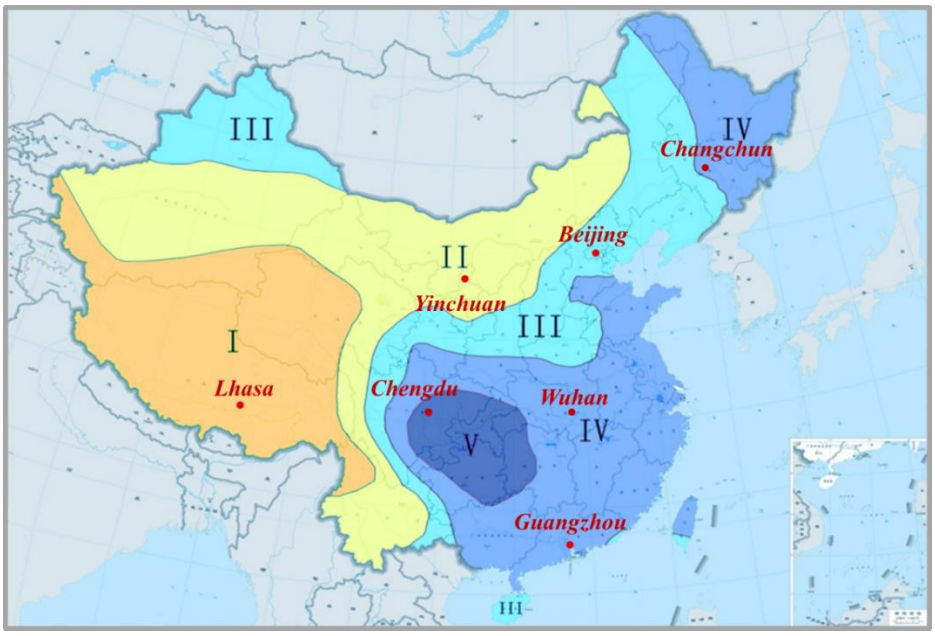

***Fig. 1**: Daylight (solar) climate zones and seven locations in China.*

***Table 2**: Daylight (solar) climate zones, annual-averaged illuminances (Eq), and locations in China* (Ministry of Housing and Urban-Rural Development, 2013).

Zone Number	**I**	**II**	**III**	**IV**	**V**
Range of annual-averaged unobstructed illuminance, Eq (klx)	≥28	[26 28)	[24 26)	[22 24)	<22
Location	Lhasa	Yinchuan	Beijing	Guangzhou, Wuhan, Changchun	Chengdu

2.2 Greenhouse models studied

Figure 2 presents two greenhouse models studied in this article. They have a rectangular plan with a dimension of 15 × 40 m (length × width) and an area of 600 m^2. The greenhouses have a multi-span structure and the width of each single span is 3.0 m. Two

types of roof were adopted for models respectively, including A-frame (Sharples and Lash, 2007) and Barrel-vault (Laouadi, 2005). The sections were defined across the width of greenhouses. Each section consists of two spatial parts: the roof space (height: 1.5 m) and the normal space (height: 4.2 m). Four orientations of each greenhouse were studied (see Figure 3 (a)), such as O1 (the length aligning with east-west); O2 (the length aligning with north-south); O3 (the length aligning with north-east or south-west); O4 (the length aligning with north-west or south-east). Walls and roofs of these greenhouses were set with a double-glazing envelop: it has a thickness of 24mm and two layers of 6 mm clear float glass (IGDB (International Glazing Database), 2019). Compared with single-glazing, significant energy savings can be achieved with double-glazing (Gupta and Chandra, 2002; Vadiee and Martin, 2014) and thus the double-glazing envelope has become a trending technology in many countries to increase the greenhouse performance (Harjunowibowo et al., 2016). Key solar thermal and optical properties of the glazing layer are 0.656 (solar heat transmittance) and 0.801 (visual transmittance) (Ministry of Agriculture and Rural Affairs of China, 2012). The inside floor was set as the typical ground material (grey soil, reflectance: 0.2).

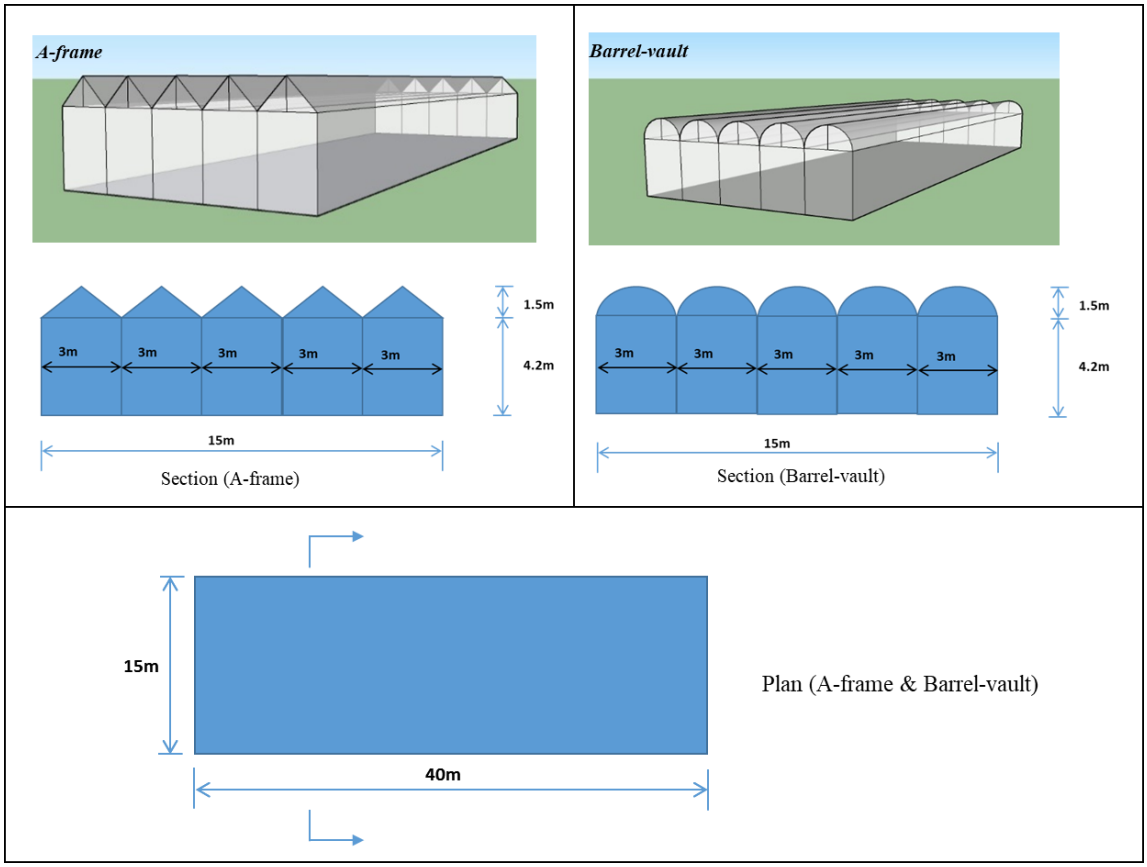

Fig. 2: *Two types of greenhouse models and their configurations and dimensions.*

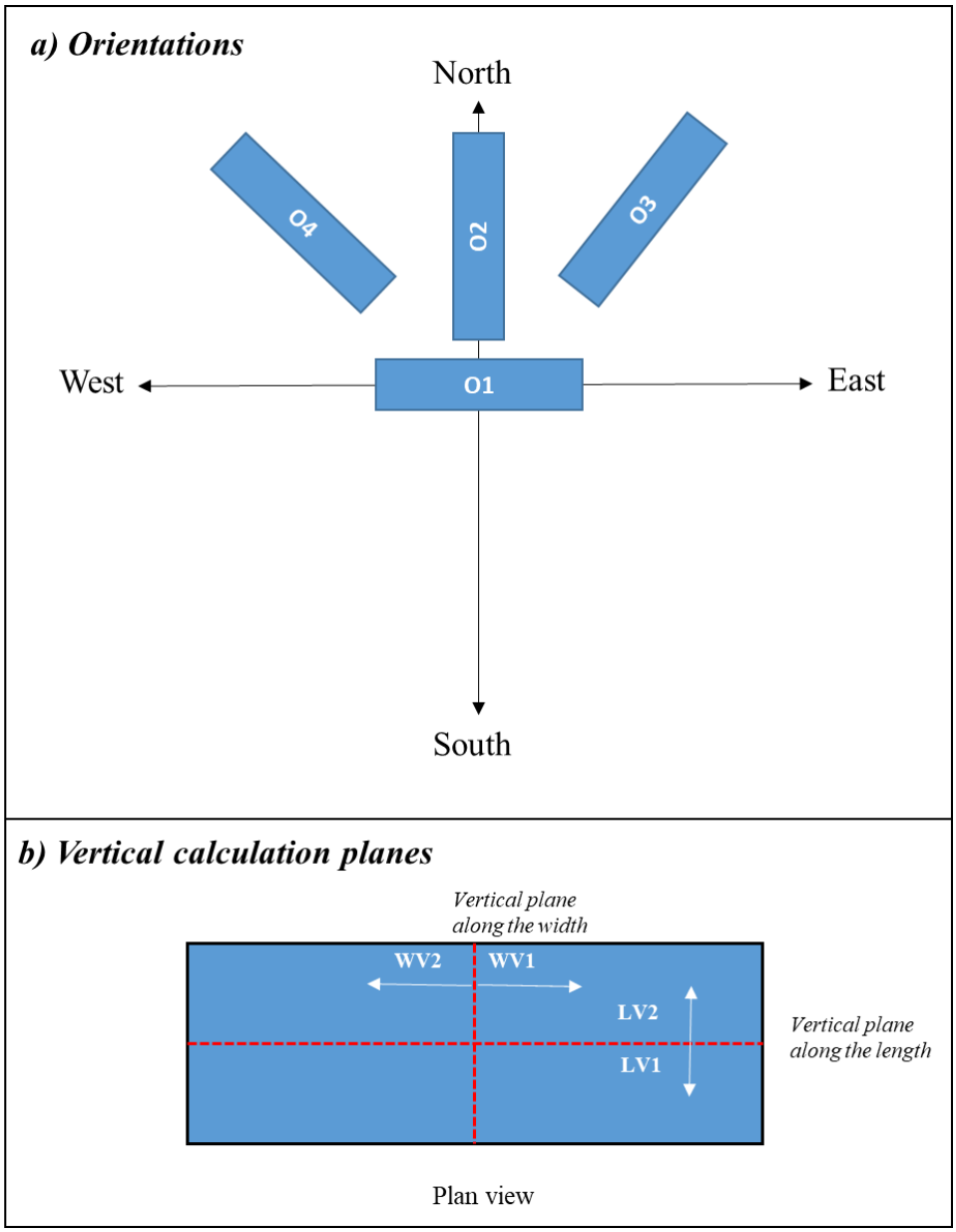

Fig. 3: *Orientations and the vertical calculation planes for PAR analysis in two greenhouse models.*

2.3 Photosynthetically Active Radiation

Photosynthetically active radiation (PAR) is a portion of solar radiation that can be utilized by green plants in the process of photosynthesis (Hall and Rao, 1999). Technically,

PAR is defined as the solar radiation in a spectral range of 400 and 700 nm. Given the studies of plant science, PAR can be expressed in terms of solar irradiance (W/m^2) or photosynthetic photon flux density (PPFD), i.e. the number of photons incident per unit time on a unit surface (μmol/m^{2}s) (Sun et al., 2017). The monochromatic relationship between the aforementioned two quantities can be given through Eq. 1:

$$P_\lambda = \frac{F_\lambda \lambda}{N_A hc} \quad (1),$$

where, P_λ means the PPFD, F_λ is the solar irradiance, λ is the wavelength, N_A is the Avogadro constant, h is the Planck constant, and c is the speed of light. Photons of PAR wavelength will be absorbed by the green plants as a source of energy in the process of photosynthesis and are thus important for the plant growth. In addition, it can be found from Eq. 1 that the photon flux depends explicitly on the wavelength and therefore the photon flux cannot be directly derived from the solar irradiance. In climate studies, PAR values are often estimated based on the global solar irradiance using the following empirical equation (Dong et al., 2011; Zhou et al., 2013):

$$Q_{PAR} = \eta_0 Q \quad (2),$$

where Q_{PAR} is PAR expressed in W/m^2, Q denotes the global solar irradiance and η_0 is the ratio measured based on the climate conditions.

2.4 Simulations

Developed for daylight/solar simulations, RADIANCE has been recognized as an accurate tool to calculate the global solar irradiation (W/m^2) under various sky conditions ("RADIANCE," 2020). Using a hybrid approach of Monte-Carlo and deterministic ray-

tracing, RADIANCE simulation starts at a measurement point and traces rays of light backwards to the sources. The radiance values, i.e. the amount of light passing a specific point in a specific direction, can be calculated, including the direct component, the specular indirect component and the diffuse indirect component. Combined with the Perez all-weather sky model (Perez et al., 1993, 1990), RADIANCE has become one of the most commonly used computer programmes for daylight simulations under real sky conditions. Validation studies have shown that the RADIANCE results are in good agreement with measurements and theoretical analyses (Mardaljevic, 1995; Reinhart and Walkenhorst, 2001). One of the authors of the present study had successfully employed RADIANCE to investigate the daylight availability in buildings (Du, 2011; Lu and Du, 2019).

In order to evaluate the PAR availability, this study first employed RADIANCE to calculate the global solar irradiance received inside the greenhouses. Then, PAR values were obtained through the Eq. 2. The value of η_0 in Eq. 2 slightly varies in locations, seasons, and other meteorological parameters (Janjai et al., 2015). This study adopted $\eta_0 = 0.44$, which is a typical value applied for the seven Chinese locations (Zhou et al., 2013).

In this study, two types of calculation positions in the greenhouses to justify the PAR availability were considered: horizontal and vertical planes. The horizontal calculation plane was set with a height of 2.1 m above the greenhouse floor (the normal direction is upward), which was defined at the half height of normal space in greenhouses to represent

the horizontal PAR availability. As shown in Figure 3(b), four vertical calculation planes were positioned cross the greenhouse center along the length (LV1 & LV2) and the width (WV1 & WV2) (the normal directions were marked using white arrowheads). Only the PAR availability in the normal space of greenhouses (lower than 4.2 m) was analyzed. These calculation planes can be used to indicate the PAR levels in the greenhouses with various vertical planting system.

3. Results

This section has three parts with the analysis of PAR availability: effects of greenhouse roofs, effects of orientations, and effects of locations and climates.

3.1 Effects of greenhouse roofs

The monthly-averaged hourly PAR (Alados et al., 1996) have been evaluated in four typical months (December, March, June, and September) and with two roofs: A-frame (A-roof) and Barrel-vault (B-roof). Lhasa, Beijing, and Chengdu were studied here as representatives of locations with high, medium, and low levels of solar availability. Since this section focuses on the roof effect, only the orientation O1 was included in the analysis.

3.1.1 PAR availability at horizontal plane

Figure 4 gives comparisons of PAR availability at the horizontal plane between two roofs in Lhasa (a), Beijing (b) and Chengdu (c). Taking the A-frame model as a reference, the relative difference of PAR between two roofs (R_{roofh}) can be quantified according to the following equation:

$$R_{roofh} = \frac{\overline{PAR}_{h,B} - \overline{PAR}_{h,A}}{\overline{PAR}_{h,A}} \times 100\% \quad (3),$$

where $\overline{PAR}_{h,A}$ and $\overline{PAR}_{h,B}$ denote the average PAR received at the horizontal plane during the working time (6:00—18:00) with A-roof and B-roof respectively.

Generally, A-roof greenhouses have similar PAR varying trends as B-roof greenhouses at three cities, whilst there are no big differences of PAR levels at the horizontal plane between two roofs (absolute $R_{roofh} < 10\%$). The relative difference of annual PAR ranges from -2.64% in Lhasa to -1.29% in Chengdu. Given the variation in different seasons (Figure 4), it seems that roof effects vary in locations. At Lhasa, for instance, B-roof greenhouses receive 7.84% less PAR than A-roof in winter (December), whereas A-roof greenhouses achieve slightly higher PAR than B-roof models in other months. However, for Chengdu, no significant differences of PAR can be found between two roofs cross the year.

a) Lhasa

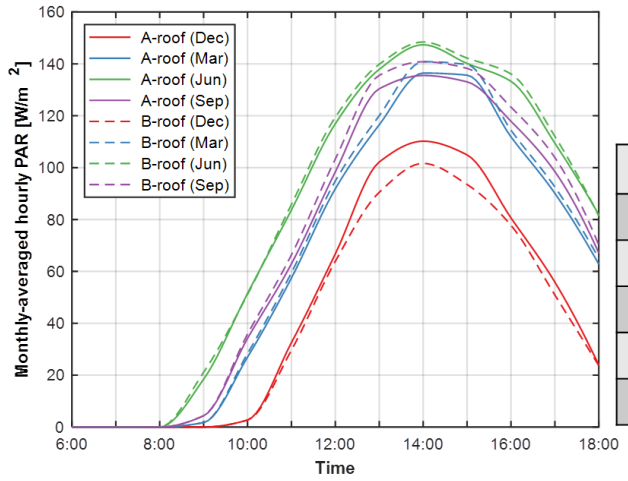

Relative difference of PAR (R_{roofh}) between two roofs	
December	-7.84%
March	3.10%
June	1.66%
September	4.50%
Annual	-2.64%

b) Beijing

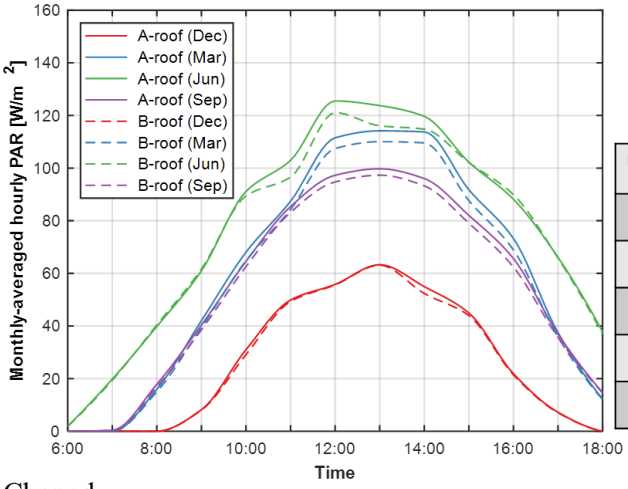

Relative difference of PAR (R_{roofh}) between two roofs	
December	-2.10%
March	-4.26%
June	-2.42%
September	-3.19%
Annual	-1.83%

c) Chengdu

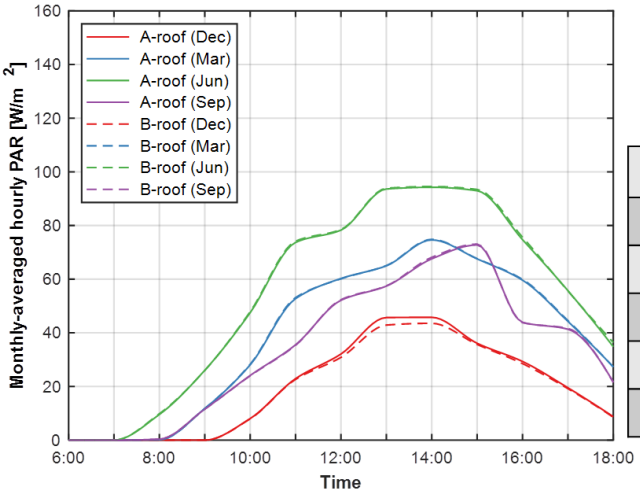

PAR relative difference between two roofs	
December	-3.38%
March	0.30%
June	0.70%
September	0.19%
Annual	-1.29%

Fig. 4: *Comparison of PAR availability at the horizontal plane between two roofs and with the orientation (O1) in Lhasa (a), Beijing (b), and Chengdu (c).*

3.1.2 PAR availability at vertical plane

Figure 5 & 6 present comparisons of PAR availability between two roofs at the vertical planes LV1 & LV2, and vertical planes WV1 & WV2 respectively. The relative difference of vertical PAR between two roofs (R_{roofv}) is defined by:

$$R_{roofv} = \frac{\overline{PAR}_{v,B} - \overline{PAR}_{v,A}}{\overline{PAR}_{v,A}} \quad (4),$$

where $\overline{PAR}_{v,A}$ and $\overline{PAR}_{v,B}$ are the average PAR at the vertical planes with two roofs.

Similar to the horizontal plane, PAR levels of A-roof vary in the same trends at vertical planes as B-roof models. It can also be found that there are generally few differences of vertical PAR levels between two roofs (absolute R_{roofv} < 5%). For vertical planes LV1 & LV2, average PAR levels decrease by only 1.72% in Lhasa, 1.91% in Beijing, and 2.36 % in Chengdu when A-roof is replaced by B-roof. With vertical planes WV1 & WV2, the relative differences of PAR are -1.60% (Lhasa), -1.09% (Beijing), and -1.13% (Chengdu). Effects of roof on PAR availability at vertical planes might also linked to the seasonal and locational factors. Relative differences of PAR between two roofs are slightly larger in winter than that in summer at all locations. A special case can be found in Lhasa. For instance, B-roof greenhouse may see slightly higher PAR than A-roof models in summer (June).

a) Lhasa

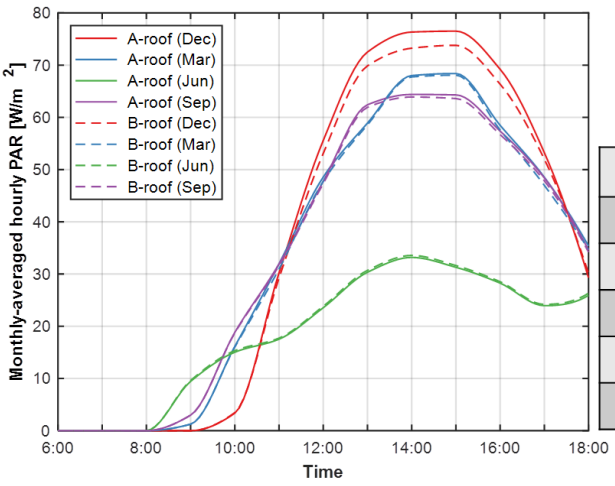

Relative difference of PAR (R_{roofv}) between two roofs	
December	-3.24%
March	-1.37%
June	1.25%
September	-0.96%
Annual	-1.72%

b) Beijing

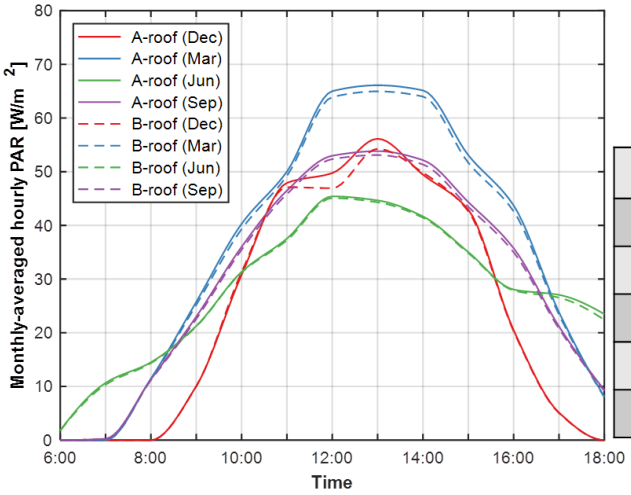

Relative difference of PAR (R_{roofv}) between two roofs	
December	-1.66%
March	-1.98%
June	-1.07%
September	-1.59%
Annual	-1.91%

c) Chengdu

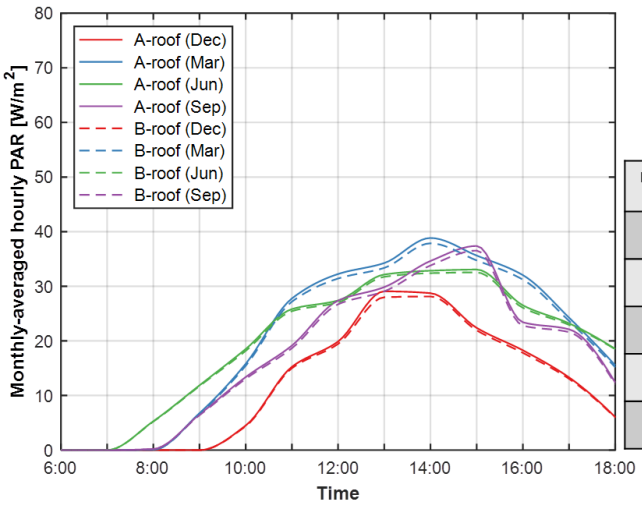

Relative difference of PAR (R_{roofv}) between two roofs	
December	-2.41%
March	-2.45%
June	-1.36%
September	-2.42%
Annual	-2.36%

Fig. 5: *Comparison of PAR availability at the vertical plane (LV1 & LV2) between two roofs and with the orientation (O1) in Lhasa (a), Beijing (b), and Chengdu (c).*

a) Lhasa

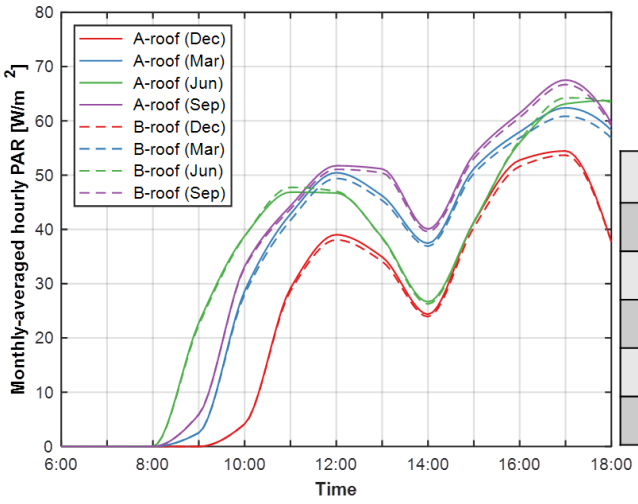

Relative difference of PAR (R_{roofv}) between two roofs	
December	-1.79%
March	-2.09%
June	0.25%
September	-1.18%
Annual	-1.60%

b) Beijing

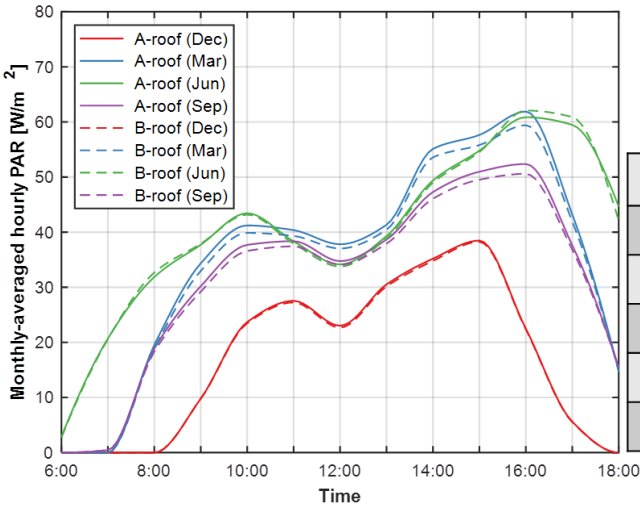

Relative difference of PAR (R_{roofv}) between two roofs	
December	-0.94%
March	-2.98%
June	-0.24%
September	-2.54%
Annual	-1.09%

c) Chengdu

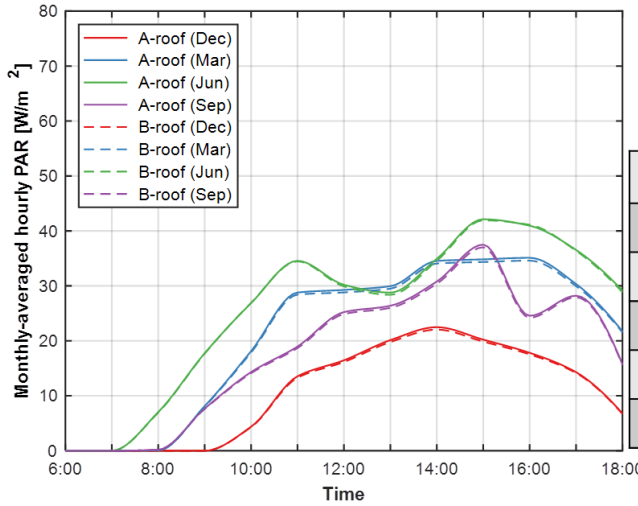

Relative difference of PAR (R_{roofv}) between two roofs	
December	-1.69%
March	-1.34%
June	-0.52%
September	-1.28%
Annual	-1.13%

Fig. 6: *Comparison of PAR availability at the vertical plane (WV1 & WV2) between two roofs and with the orientation (O1) in Lhasa (a), Beijing (b), and Chengdu (c).*

3.1.3 Summary

It can be found that roof configurations would not be able to affect PAR variations and levels at both horizontal and vertical planes in greenhouses. Even though Lhasa sees a relatively higher difference (7.84%), most of locations share the same trend. Thus, only A-roof was considered when investigating the effect of orientation and climate on the PAR availability in the following sections.

3.2 Effect of orientations

This section focuses on effects of greenhouse orientation on the PAR availability. Similar to section 3.1, this analysis only includes three cities (Lhasa, Beijing, and Chengdu) and four typical months (December, March, June, and September). Given the insignificant difference of PAR between A-frame and Barrel-vault roofs, only greenhouses with A-frame roof were analysed.

3.2.1 PAR availability at horizontal plane

Figure 7 shows hourly PAR variations at the horizontal plane with four orientations. The general trends of PAR variations at the horizontal plane are similar between four orientations. The PAR peaks between 12:00–15:00 for all locations and orientations. It can be noted that PAR differences caused by orientations tend to be larger after 12:00, especially at Lhasa and Beijing. In Lhasa, December can see orientation O2 receives 12.6% less PAR around 14:00 than orientation O1, while achieves higher PAR levels than O1 after 16:00. For Chengdu, the orientation takes unclear effect on PAR variation across the working time.

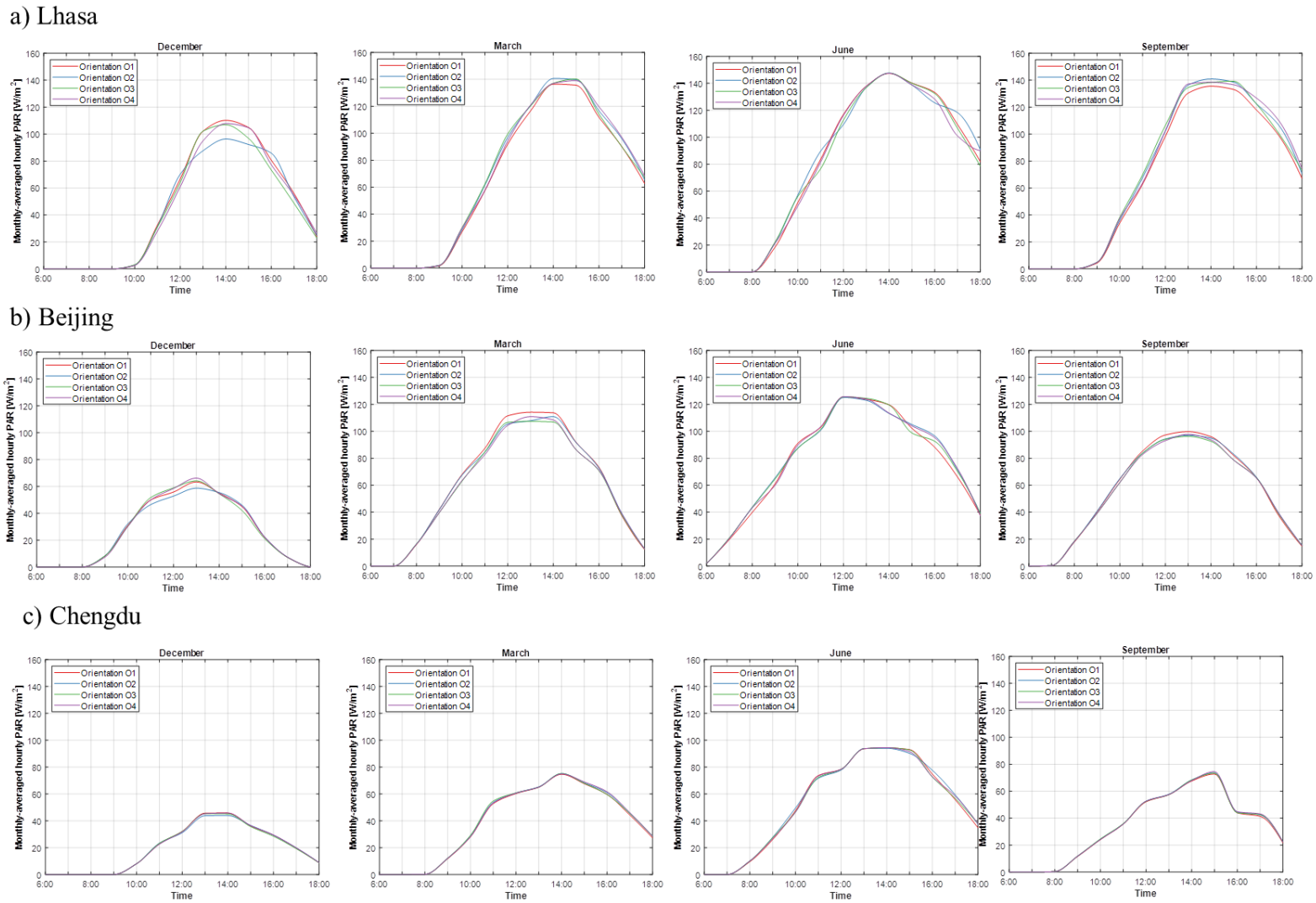

Fig. 7: *PAR availability at the horizontal plane with A-frame roof and four orientations (O1, O2, O3, and O4) in Lhasa, Beijing, and Chengdu.*

***Table 3**: Relative difference of monthly PAR (R_{oh}) at the horizontal plane of greenhouse with three orientations (O2, O3 and O4) and A-frame roof, taking the orientation O1 as a reference (locations: Lhasa, Beijing, and Chengdu; working time: 6:00-18:00).*

Relative Difference (R_{oh})				
Location	**Period**	**Orientation (O2)**	**Orientation (O3)**	**Orientation (O4)**
Lhasa	December	-5.98%	-5.31%	-3.90%
	March	4.41%	3.82%	4.11%
	June	1.50%	-1.06%	-0.88%
	September	4.97%	5.07%	5.58%
	Annual	0.10%	-0.95%	-0.48%
Beijing	December	-2.35%	0.26%	1.30%
	March	-2.19%	-4.58%	-4.27%
	June	1.43%	1.00%	1.14%
	September	-0.49%	-2.36%	-2.23%
	Annual	-0.31%	-0.73%	-0.34%
Chengdu	December	-1.43%	-0.99%	-0.12%
	March	1.50%	1.43%	1.58%
	June	1.12%	0.19%	0.29%
	September	1.27%	1.14%	1.48%
	Annual	0.57%	0.17%	0.56%

To effectively compare effects of orientation on PAR performance, the relative difference of monthly PAR at the horizontal plane (R_{oh}) was calculated for orientations O2, O3, and O4, taking Orientation O1 as a reference:

$$R_{oh} = \frac{\overline{PAR}_{h,o_i} - \overline{PAR}_{h,o_1}}{\overline{PAR}_{h,o_1}} \quad (5),$$

where $\overline{PAR}_h$ is monthly- or annual-averaged PAR at the horizontal plane; $i = 2, 3, or\ 4$ representing the corresponding orientations. R_{oh} values are presented in Table 3. Lhasa and Beijing can receive slightly higher R_{oh} values in December, March and September. For example, the maximum R_{oh} values can reach nearly -6% in Lhasa (O2 in

December) and -4.58% in Beijing (O3 in March). However, similar to Figure 7 (c), Chengdu has no big PAR differences between orientations since all absolute R_{oh} values < 2%.

3.2.2 PAR availability at vertical plane

Figure 8 & 9 present comparisons of PAR availability between four orientations at vertical planes LV1 & LV2 and WV1 & WV2 respectively. Different from the horizontal PAR in Figure 7, variations of hourly vertical PAR show significant impact from orientations here.

Vertical PAR peaks at different times and dates under different orientations. At vertical plane LV1 & LV2 (Figure 8), orientation O3 sees PAR tends to peak first, followed by O1. The latest peak time is found with orientation O4. It is worth noting that the PAR under orientation O2 shows two peaks occurring in the morning and afternoon. There is valley of PAR variation in between the two peaks, whose time is roughly the same as the peak time of orientation O1. In Lhasa, the PAR at vertical planes LV1 & LV2 reaches the highest level at around 14:00 under orientation O1, whereas under orientation O2 the PAR peaks twice at around 12:00 and 17:00. A similar trend can be also observed in Beijing, but cannot be clearly found in Chengdu. Orientation O1 tends to receive the highest PAR level of PAR in December (winter), whereas orientation O2 has the greatest potential of PAR application in June (summer). When comparing O3 with O4, orientation O3 has slightly higher PAR levels at the vertical plane LV1 & LV2. For vertical plane WV1 & WV2 (Figure 9), it is normal to see a reversed trend according to PAR variations

in contrast to LV1 & LV2. Orientation O4 shows the earliest peak time, while the PAR of orientation O3 peaks at the latest time. Similarly, two PAR peaks are observed with orientation O1. Orientation O2 and orientation O1 achieve the highest PAR in December and June respectively. A higher PAR levels can be delivered with orientation O4 than orientation O3.

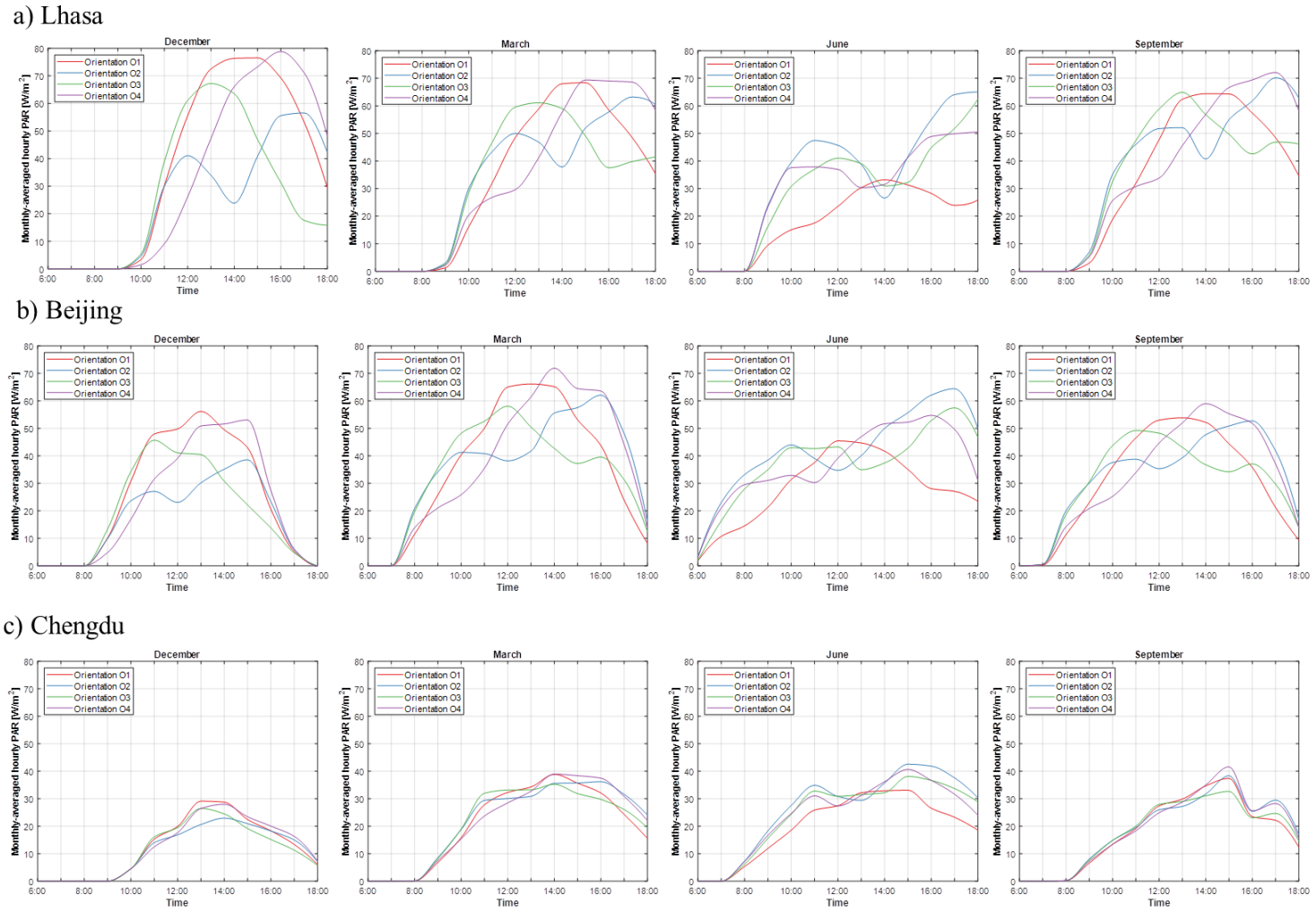

Fig. 8: *PAR availability at the vertical plane (LV1 & LV2) with A-frame roof and four orientations (O1, O2, O3, and O4) in Lhasa (a), Beijing (b), and Chengdu (c).*

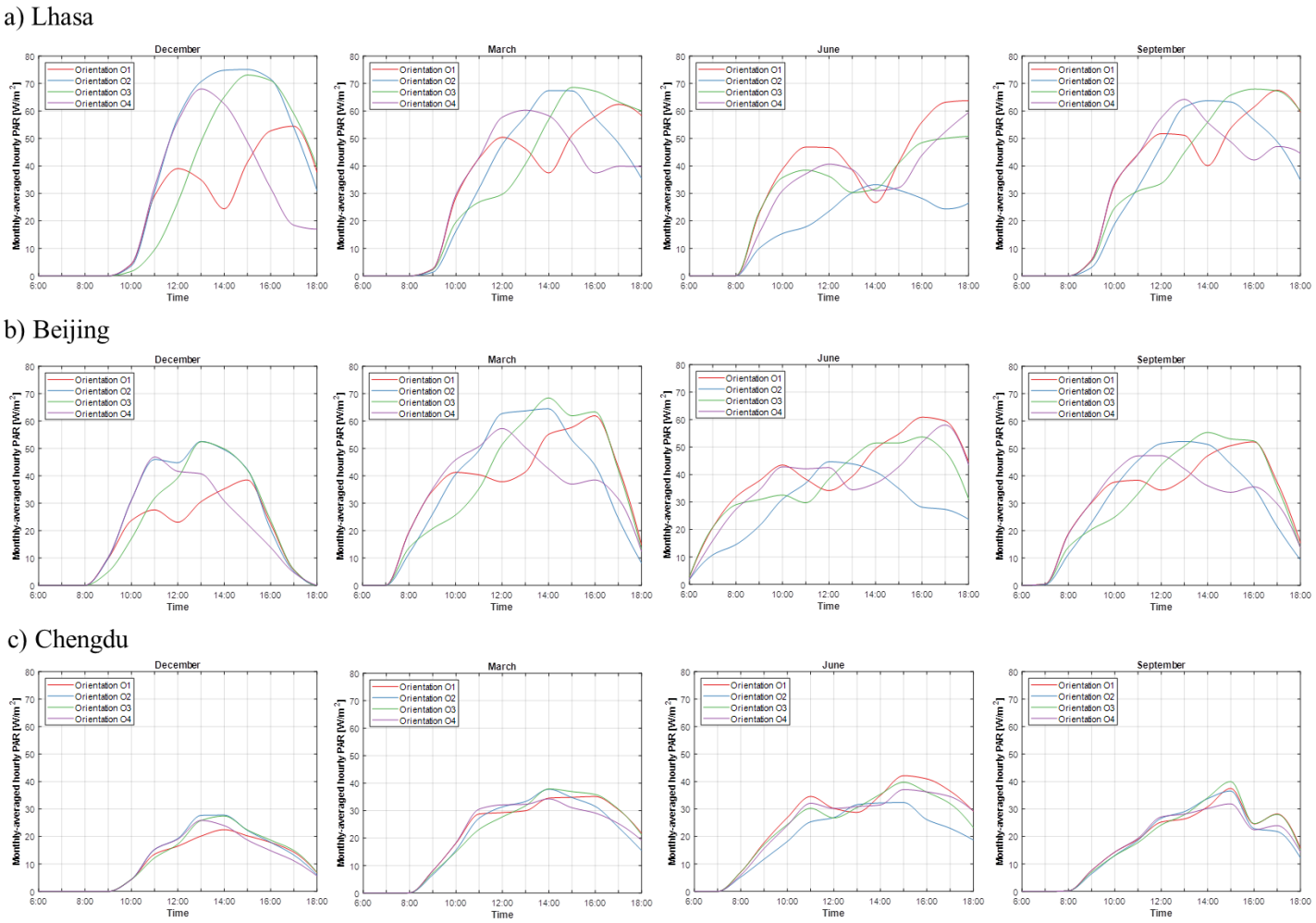

Fig. 9: *PAR availability at the vertical plane (WV1 & WV2) with A-frame roof and four orientations (O1, O2, O3, and O4) in Lhasa (a), Beijing (b), and Chengdu (c).*

The relative difference of vertical PAR levels between orientations ($\mathbf{R_{ov}}$) is defined by:

$$R_{ov} = \frac{\overline{PAR}_{v,o_i} - \overline{PAR}_{v,o_1}}{\overline{PAR}_{v,o_1}} \quad (6),$$

where $\overline{PAR}_v$ denote the monthly- or annual-averaged PAR at the vertical planes, $i = 2, 3, or\ 4$ representing the corresponding orientations. The values of R_{ov} are presented in Table 4 and 5 for vertical planes LV1 & LV2, and WV1 & WV2 respectively. Absolute $\mathbf{R_{ov}}$ values are significantly higher in December (winter) and June (summer) than in March (spring) and September (autumn). These values range from 1% to 10% for March and September, while reach 47.47% in December and 87.58% in June. For vertical planes LV1 & LV2 (Table 4), December (winter) sees the maximum monthly PAR with orientation O1, whilst June (summer) has the maxima with orientation O2. As for locations, the maximum values of R_{ov} at the two planes are 87.58% and 48.26% in Lhasa and Beijing respectively. Compared with Lhasa and Beijing, R_{ov} values are lower in Chengdu and the maximum absolute R_{ov} is around 32% (June). On the other hand, vertical planes WV1 & WV2 (Table 5) receive the maximum monthly PAR with orientation O1 in summer (June) and orientation O2 in winter (December). The maximum values of R_{ov} for Lhasa and Beijing are 47.47% and 39.37% respectively. In Chengdu, the maxima of R_{ov} can just reach around 30%.

***Table 4**: Relative difference of monthly PAR (R_{olv}) at the vertical plane (LV1 & LV2) of greenhouse with three orientations (O2, O3 and O4) and A-frame roof, taking the orientation O1 as a reference (locations: Lhasa, Beijing, and Chengdu; working time: 6:00-18:00).*

Relative Difference (R_{olv})				
Location	**Period**	**Orientation (O2)**	**Orientation (O3)**	**Orientation (O4)**
Lhasa	December	-29.52%	-25.37%	-9.62%
	March	2.03%	-2.35%	1.75%
	June	87.58%	61.96%	62.74%
	September	11.42%	4.31%	7.24%
	Annual	8.27%	1.82%	8.12%
Beijing	December	-30.74%	-21.28%	-10.07%
	March	0.78%	-5.55%	3.08%
	June	48.26%	32.93%	30.48%
	September	6.38%	-0.38%	5.56%
	Annual	5.30%	0.27%	6.59%
Chengdu	December	-11.17%	-9.77%	-1.01%
	March	6.59%	1.68%	4.57%
	June	31.63%	21.63%	20.21%
	September	4.88%	-0.35%	5.35%
	Annual	10.65%	4.43%	8.56%

***Table 5**: Relative difference of monthly PAR (R_{owv}) at the vertical plane (WV1 & WV2) of greenhouse with three orientations (O2, O3 and O4) and A-frame roof, taking the orientation O1 as a reference (locations: Lhasa, Beijing, and Chengdu; working time: 6:00-18:00).*

Relative Difference (R_{owv})				
Location	**Period**	**Orientation (O2)**	**Orientation (O3)**	**Orientation (O4)**
Lhasa	December	47.47%	24.17%	6.87%
	March	-1.52%	-0.60%	-4.77%
	June	-45.95%	-13.19%	-14.11%
	September	-8.20%	-2.64%	-5.35%
	Annual	-6.73%	-0.77%	-5.92%
Beijing	December	39.37%	23.31%	11.95%
	March	0.01%	1.86%	-6%
	June	-30.47%	-9.93%	-8.34%
	September	-5.11%	-0.77%	-6.15%
	Annual	-3.55%	1.99%	-3.23%
Chengdu	December	12.81%	10.13%	1.95%
	March	-4.87%	-1.28%	-3.91%
	June	-23.60%	-8.06%	-6.57%
	September	-3.66%	1.04%	-4.31%
	Annual	-8.80%	-1.41%	-4.58%

3.2.3 Summary

In sum, effects of orientation on the PAR availability are substantially clear at the vertical planes, while the horizontal plane shows the insignificant impact of orientation. The general varying trends are similar between four orientations at the three cities. Effects of orientation on the vertical PAR are much clearer in Lhasa and Beijing than in Chengdu. The PAR availability is more sensitive to the greenhouse orientation in winter and summer than in spring and autumn.

3.3 Effect of locations and climates

This section focuses on effects of locations and climates on the PAR availability. Thus, seven locations have been included in this section. Similarly, only greenhouses with A-frame roof and orientation O1 were analysed.

3.3.1 Variations of monthly averaged PAR

Table 6 indicates the monthly-averaged PAR at the horizontal plane. It can be found that there are clear seasonal variations of horizontal PAR at seven locations. Lhasa (Zone I) generally has the highest PRA levels across the year, although the maximum monthly PAR occurs in Yinchuan in June (83.0 W/m^2). Yinchuan (Zone II) receives higher PAR levels than Beijing (Zone III) from April to July, while sees a similar PAR level as Beijing in other periods. The monthly PAR peaks in the same period from May to July in Lhasa, Yinchuan, and Beijing. For three locations in Zone IV such as Guangzhou, Wuhan, and Changchun, PAR peaks in the periods from July to October, from July to August, and from May to June respectively. Compared with Wuhan and Changchun, Guangzhou tends to receive more PAR in autumn and winter and less PAR in spring and summer. In winter (from November to December), Guangzhou can even achieve the similar PAR level as Lhasa. In May and June, Changchun has a PAR level similar to the value of Beijing, which is significantly higher than Wuhan and Guangzhou. However, Changchun has the lowest PAR level from November to January among seven locations. Chengdu (Zone V) generally has the lowest PAR level across the year, although a slightly higher PAR level can be found here in spring than Guangzhou (Zone IV).

***Table 6**: Monthly-averaged PAR at the horizontal plane of greenhouse with O1 orientation, A-frame roof and seven locations (working time: 6:00-18:00).*

Monthly averaged horizontal PAR												
Location \ Month	1	2	3	4	5	6	7	8	9	10	11	12
Lhasa	47.6	60.7	64.0	76.9	82.1	78.5	80.0	75.0	67.9	62.9	49.4	44.6
Yinchuan	29.8	41.0	56.2	70.0	76.7	83.0	77.0	66.5	59.6	49.3	34.7	27.9
Beijing	29.0	45.2	59.1	69.2	70.8	75.4	67.2	66.7	53.9	43.9	31.9	25.9
Guangzhou	36.8	35.0	31.9	41.6	54.7	49.2	59.8	57.9	57.1	58.5	49.1	43.3
Wuhan	28.9	35.9	41.7	52.2	56.4	60.9	67.3	64.9	50.4	41.0	35.3	29.2
Changchun	19.3	31.0	43.7	62.3	73.0	73.7	62.9	58.1	52.7	34.8	20.3	15.7
Chengdu	21.1	22.8	37.8	47.7	51.8	52.4	55.1	54.6	33.0	32.6	23.2	19.1

The monthly-averaged PAR values at the vertical planes LV1 & LV2 and WV1 & WV2 are given in Table 7 and 8. Compared with the horizontal plane (Table 6), the monthly PAR at vertical planes LV1 & LV2 shows different seasonal variations (Table 7). Clearly, differences between vertical PAR values in various months tend to be lower. In Lhasa (Zone I), summer (June) sees the lowest vertical PAR level in a year, while the highest vertical PAR levels are found in the period from October to February. The trend that spring and autumn have similar vertical PAR levels as summer and winter can be observed in locations including Yinchuan (Zone II), Beijing (Zone III), Wuhan and Guangzhou (Zone IV). With the exception of winter, Changchun (Zone IV) has a relatively higher level of PAR than Guangzhou and Wuhan for other seasons. For Chengdu (Zone V), vertical PAR levels in spring, summer and autumn are higher than in winter. For vertical planes WV1 & WV2 (Table 8), the monthly-averaged PAR varies in a similar trend as the

horizontal plane (see Table 6), while the range of vertical PAR is smaller than the horizontal PAR. As shown in Table 8, the monthly PAR starts to increase from January and peaks in the summer period (from May to August), and then decreases towards December. The maximum monthly PAR occurs in June at Yinchuan (Zone II, 40.5 W/^{2}) whilst the minimum value can be found in December at Chengdu (Zone V, 10.5 W/m^2). In general, Lhasa has higher PAR levels than Yinchuan and Beijing, especially in winter. Yinchuan and Beijing have similar levels of PAR across the year. In Zone IV, Changchun sees higher PAR levels than Wuhan and Guangzhou from April to June (spring), whereas Guangzhou has higher PAR levels in the winter period (from October to January). The PAR levels in Chengdu (Zone V) are generally the lowest among seven locations.

Table 7: *Monthly-averaged PAR at the vertical plane (LV1 & LV2) of greenhouse with O1 orientation, A-frame roof and seven locations (working time: 6:00-18:00).*

Monthly vertical averaged PAR (LV1 & LV2)												
Month / Location	1	2	3	4	5	6	7	8	9	10	11	12
Lhasa	35.5	37.7	33.5	31.1	24.7	18.3	23.0	26.3	33.3	36.6	34.8	35.9
Yinchuan	27.0	29.4	31.8	32.7	30.8	32.5	30.6	29.8	31.4	33.1	29.5	26.9
Beijing	26.9	33.8	34.8	34.1	27.7	27.9	26.7	31.4	29.7	28.9	26.8	24.0
Guangzhou	23.1	20.0	16.8	20.5	24.1	21.1	26.2	24.1	27.8	31.7	30.2	28.8
Wuhan	19.4	21.6	22.0	25.1	21.6	23.6	22.1	28.8	25.7	24.1	23.7	20.3
Changchun	20.5	25.8	28.5	33.1	32.7	31.5	29.1	28.7	31.6	26.3	19.7	17.4
Chengdu	13.6	13.2	20.3	23.0	22.5	19.6	23.4	24.1	17.4	18.8	14.4	12.1

***Table 8**: Monthly-averaged PAR at the vertical plane (WV1 & WV2) of greenhouse with O1 orientation, A-frame roof and seven locations (working time: 6:00-18:00).*

Monthly averaged vertical PAR (WV1 & WV2)												
Month / Location	1	2	3	4	5	6	7	8	9	10	11	12
Lhasa	25.7	32.4	33.7	38.8	38.1	34.2	36.9	35.6	36.1	33.2	25.4	24.5
Yinchuan	18.0	22.7	29.3	36.6	38.1	40.5	38.7	34.7	30.5	26.8	20.1	17.3
Beijing	18.4	26.5	34.4	39.8	37.1	39.8	35.2	37.2	31.0	24.9	19.1	16.6
Guangzhou	21.3	19.0	17.6	22.2	29.2	25.3	31.7	30.2	31.7	32.1	27.2	24.6
Wuhan	16.8	20.4	23.7	28.5	29.3	31.6	33.8	34.6	27.5	22.9	20.2	17.2
Changchun	13.0	18.9	23.3	34.3	37.7	38.3	34.5	32.0	29.6	19.9	12.5	10.8
Chengdu	12.0	12.4	20.8	25.2	26.7	25.3	28.4	28.6	17.7	18.0	12.8	10.5

3.3.2 PAR availability in greenhouse: horizontal and vertical planes

Figure 10 shows monthly-averaged hourly PAR at the horizontal plane. The horizontal PAR values of all locations peak between 12:00 and 15:00. Generally, Lhasa sees the latest peak time, i.e. around 14:00, whilst Changchun tends to have the earliest peak time (12:00-13:00). Similar peak times can be found at Beijing, Guangzhou and Wuhan. It is also noted that the PAR peak period varies slightly in seasons. The PAR peak time at Chengdu occurs between 13:00 and 14:00 in December, but is postponed to nearly 15:00 in September. Yinchuan has an earlier peak time in June and September (13:00) than that in December and March (14:00). Lhasa has the largest PAR levels across the year, whereas the lowest PAR levels are received at Chengdu (Zone V). Yinchuan achieves a comparable level of PAR as Lhasa, especially in summer. Beijing, Guangzhou, Wuhan and Changchun have a similar level of PAR, which shows some seasonal variations. Compared with Beijing (Zone III), Wuhan and Changchun (Zone IV), Guangzhou has

1 higher PAR levels in winter and lower PAR levels in summer. By contrast, Changchun
2 receives lower PAR levels in winter and higher PAR levels in summer.

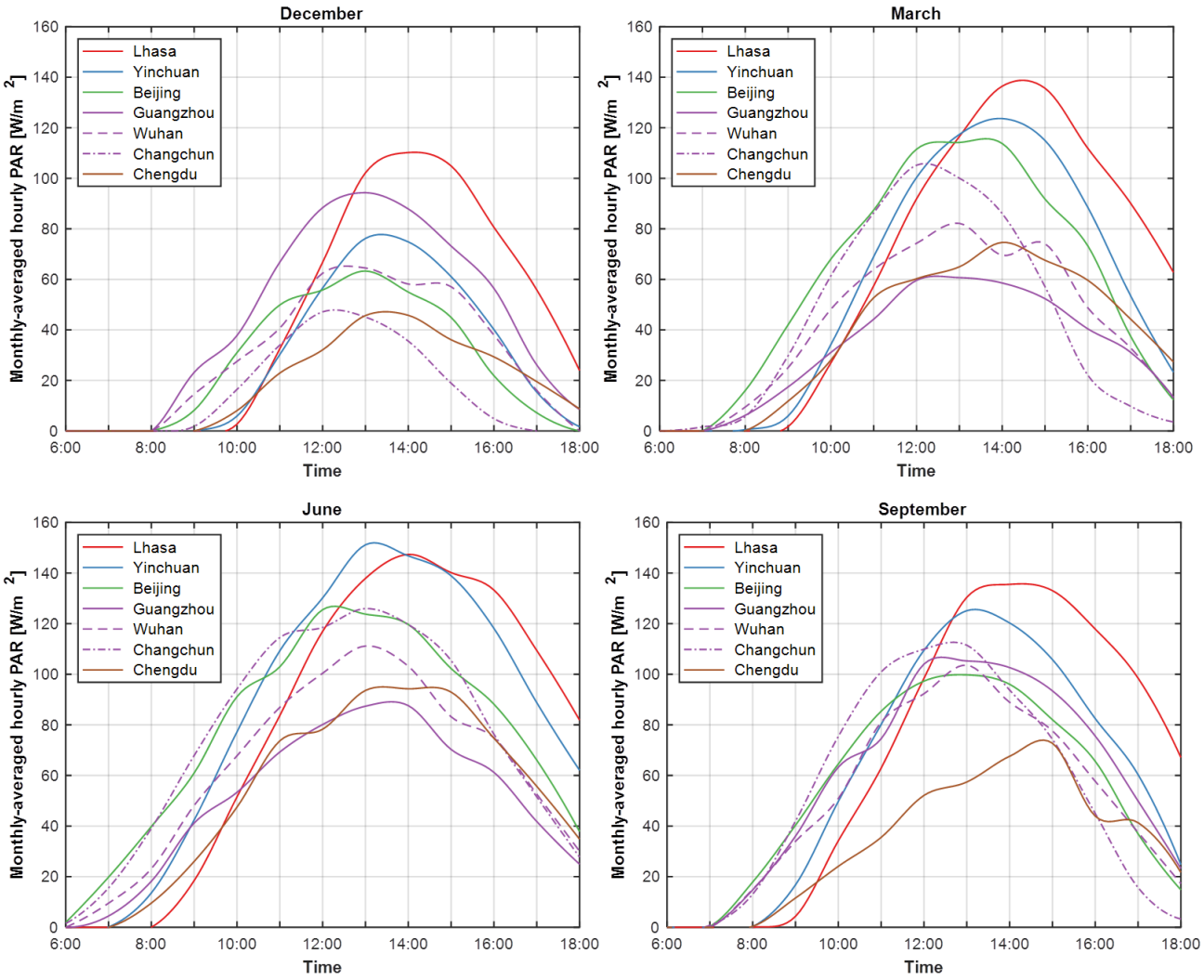

Fig. 10: *Monthly-averaged hourly PAR at the horizontal plane with A-frame roof and one orientation (O1) at seven locations.*

Figure 11 indicates monthly-averaged hourly PAR at vertical planes LV1 & LV2. The seasonal effect is clearer at the vertical planes. Similar PAR peak times can be found here as the horizontal plane. In winter (December), Lhasa and Yinchuan see higher vertical PAR levels than other locations; normally, Chengdu receives the lowest PAR levels. Interestingly, in summer (June), the low PAR levels are found in Lhasa, Wuhan, Changchun, and Chengdu, whilst Yinchuan and Changchun have higher PAR levels. Spring (March) and autumn (September) see that similar PAR levels are found between Lhasa, Yinchuan, Beijing, and Changchun, which are higher than those of Wuhan, Guangzhou, and Chengdu. Differences of PAR levels tend to be larger in winter and decrease towards the summer.

Figure 12 gives monthly-averaged hourly PAR at vertical planes WV1 & WV2. The PAR variations clearly show two peaks at Lhasa, Yinchuan, and Beijing for all seasons, with one occurring in the morning and the other found in the afternoon. There is a valley in the PAR varying trend between the two peaks. Although the peak time varies slightly in seasons, the valley time remains the same: 12:00 for Beijing, 13:00 for Yinchuan, and 14:00 for Lhasa. Chengdu still has the lowest PAR levels at these vertical planes. Lhasa, Yinchuan, and Beijing can receive the highest PAR levels. In general, compared with vertical planes LV1 & LV2, differences of PAR variations at vertical planes WV1 & WV2 tend to be smaller.

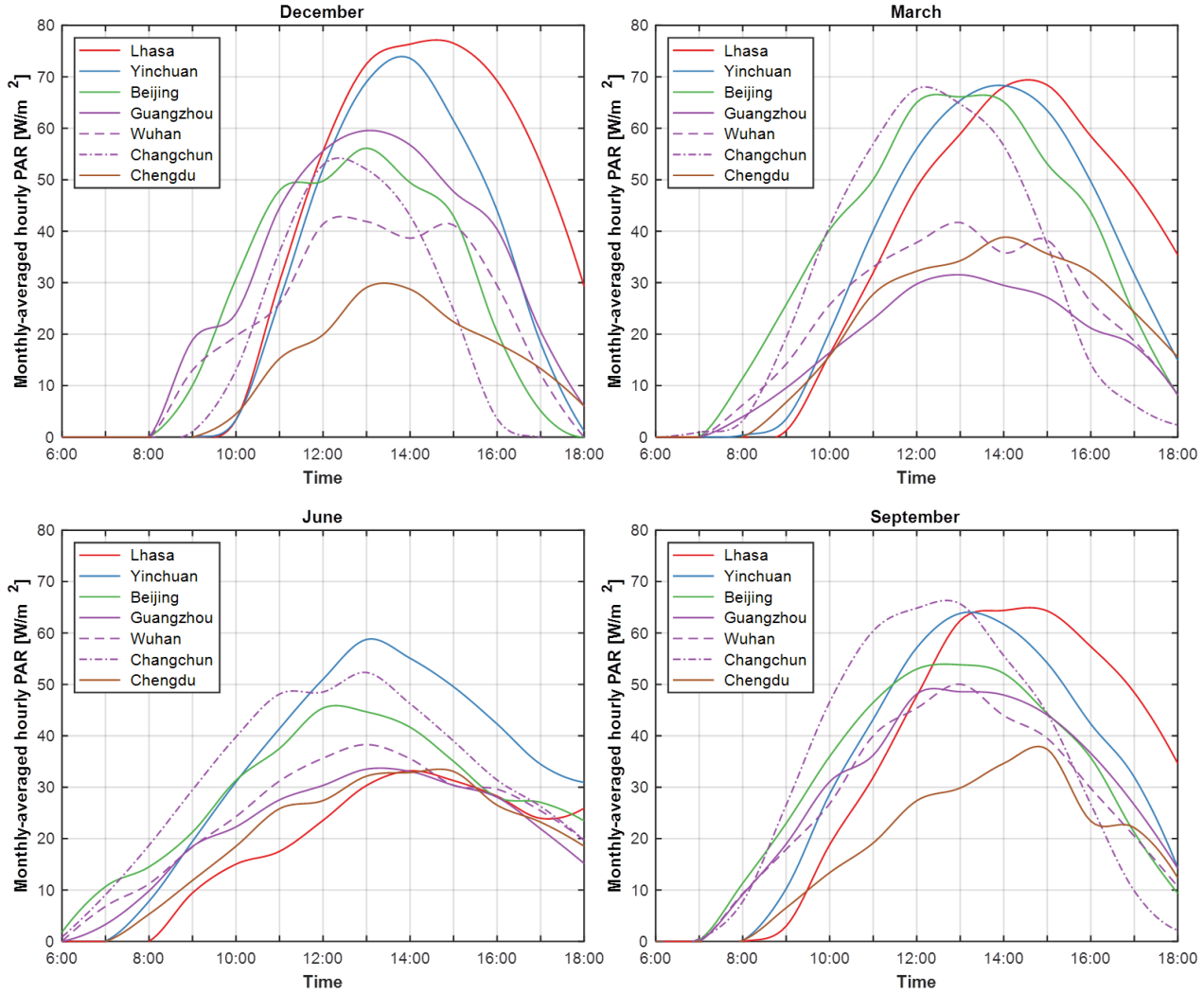

Fig. 11: *Monthly-averaged hourly PAR at the vertical plane (LV1 & LV2) with A-frame roof and one orientation (O1) at seven locations.*

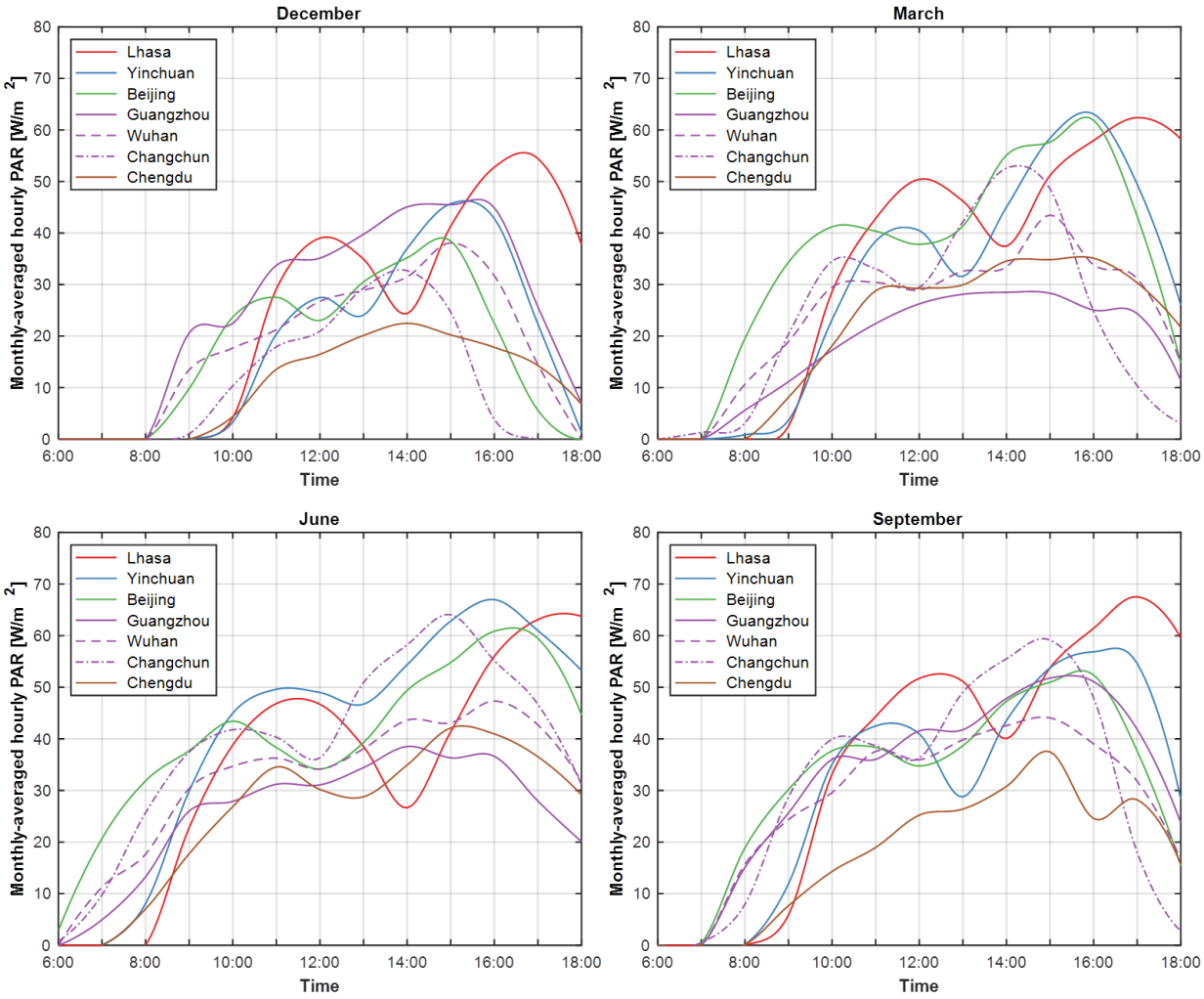

Fig. 12: *Monthly-averaged hourly PAR at the vertical plane (WV1 & WV2) with A-frame roof and one orientation (O1) at seven locations.*

3.3.3 Summary

The impact of locations and climates on PAR availability is very clear. At horizontal plane, Lhasa and Yinchuan have the highest potential to utilize PAR, while Chengdu receives the lowest PAR level. Beijing, Guangzhou, Wuhan and Changchun have a similar PAR availably. At vertical planes LV1 & LV2, Yinchuan and Chengdu have the highest and lowest PAR levels across the year respectively. However, Lhasa has the higher potential to utilize PAR at the vertical planes in winter, but not in summer. Similar to horizontal plane, other locations show medium PAR levels in between at the vertical planes. For vertical planes WV1 & WV2, similarly, Lhasa, Yinchuan and Beijing have a high PAR level and the low PAR level is found at Chengdu. Compared with vertical planes LV1 & LV2, effects of locations and climates are less clear at the vertical planes WV1 & WV2.

4. Discussions

Based on the results mentioned above, several findings are discussed as follows.

First, the present study found that effects of roof configurations (A-frame or Barrel-vault) on PAR are unclear at both horizontal and vertical planes in our greenhouse models. These roof configurations would not be able to significantly affect either overall PAR levels or PAR variations at these positions. This finding is different from the ones made in previous research works that evaluated the solar heat gains (Çakır and Şahin, 2015; Sethi, 2009; Singh and Tiwari, 2010). Such a difference is caused by the structure and envelop materials of greenhouses: the greenhouses in the present study are large-scale commercial greenhouses with both walls and roofs covered by glasses with high visual transmittance,

whereas the greenhouses in previous studies had sidewalls made of non-transparent materials. A considerable portion of sunlight received in the greenhouse comes from the transparent sidewalls in the present study and the solar radiation was received only through the transparent roof covers in previous studies. The hourly PAR profiles show relatively big differences between the two roofs at around 12:00. This could be brought by the fact that the sunlight with higher altitudes at noon would have to go through the roof before arriving in greenhouses. As regards the location, the highest and lowest effects of roof on PAR availability are found in Lhasa and Chengdu, respectively. In addition, winter sees a relatively higher difference of roof effect than other seasons in Lhasa. These results could be explained using local climates. Clear sky is the dominant climate condition in Lhasa, while overcast sky has the highest occurrence frequency in Chengdu. In Lhasa, winter sees more sunny days than other seasons. As discussed in several studies (Laouadi, 2005; Sharples and Lash, 2007), roof shapes would take greater impact on the solar beam radiation than the diffuse or reflected radiation. A clear sky would thus enhance the sensitivity of PAR availability to roof configurations. The results demonstrate that the significance of roof configuration is largely determined by the structural design of the greenhouse and is slightly subject to local climates.

Second, with a specific type of roof, no big impact of greenhouse orientation on annual PAR availability can be found at the horizontal plane, whereas vertical planes can see significant differences caused by the greenhouse orientation. Results at the horizontal plane could again be explained by the large-scale structure combined with fully-glazed

sidewalls of greenhouse. Since there is a considerable amount of sunlight coming from four sidewalls, the orientation of greenhouse would not substantially influence the solar radiation received at the horizontal plane, especially when this position is far from roof (this study: distance = 2.1 m). Gupta (2012) also pointed out that if all the walls of the greenhouse had transparent cover, the captured solar radiation would not change much with orientation. In spite of this, it can still be noted that Orientation O1 (east-west) receives slightly more sunlight in winter and slightly less sunlight in summer than Orientation O2 (north-south), indicating that these greenhouses can capture more solar heat in winter and avoid excessive solar heat in summer. This is consistent with previous studies (Chen et al., 2020; El-Maghlany et al., 2015; Kendirli, 2006; Sethi, 2009), which supported the east-west as the optimal orientation for solar energy utilization.

For vertical planes, it is normal to find a higher sensitivity to orientation in terms of PAR availability. Vertical planes LV1 & LV2 that are south & north facing under Orientation O1 will be changed into east & west facing under Orientation O2, while the same variations are applied for WV1 & WV2. Given PAR availability at the vertical plane, Lhasa and Beijing see a higher sensitivity to orientation than Chengdu. Similarly, this can again be explained by the sky condition: Chengdu has much less sunny days than Beijing and Lhasa. The diffuse light from sky does not vary in orientation. In addition, as for seasonal variations, the vertical PAR availability is more sensitive to the greenhouse orientation in winter and summer than spring and autumn. This is because sun achieves the lowest and highest altitudes in winter and summer, respectively. The east & west

facing vertical planes thus tend to receive more sunlight in the summer morning and afternoon, whereas the winter noon sees more sunlight found at the south & north facing vertical planes. The results show that, in terms of PAR availability, the effect of greenhouse orientation shows great seasonal and climatic differences, which must be considered if 'vertical farming' is adopted.

Third, the PAR availability in greenhouses receives significant impact from both location and climate. The effect of climate on the horizontal PAR availability is clearly observed. Even though Lhasa, Chengdu, and Wuhan have similar latitudes (around 30.0° N; Figure 1), their PAR availabilities in greenhouses are significantly different. The highest and lowest occurrences of clear day in Lhasa and Chengdu lead to the highest and lowest PAR availability in the two cities, respectively. With a medium occurrence of clear day, Wuhan has a medium PAR availability in between. On the other hand, the latitude difference between Guangzhou and Changchun is clearly big (Figure 1), but the two locations have a similar level of annual PAR availability, which well corresponds with the fact that they are in the same daylight climate zone (i.e. zone IV). In general, the annual horizontal PAR availability at different locations is in accordance with the daylight climate zones in China (Figure 1 & Table 2). Despite similar levels of annual PAR availability, however, the seasonal effect is clearly seen. With more sunny days in winter, Guangzhou sees higher PAR levels than Changchun, while Changchun has higher PAR levels in summer as Guangzhou is dominated by cloudy and rainy days during this period.

The effect of latitude on the vertical PAR availability is different from the horizontal plane.

Low latitude locations tend to have lower vertical PAR availabilities, especially in summer when the solar altitudes are high. At vertical planes LV1 & LV2, Yinchuan and Chengdu generally have the highest and lowest annual PAR levels, respectively. As a location with the highest altitude, Changchun tends to have a relatively high level of PAR availably from spring to autumn. Lhasa has a very low level of PAR availability in June compared with other months. Climates also exerts clear impacts on the vertical PAR availability. The solar incidence angle approaches 90 degree at noon and thus vertical planes WV1 & WV2 are supposed to receive more PAR levels in the morning or afternoon than 12:00, which would give rise to two peaks and one valley in the hourly PAR profile for all seasons. This can be found in Lhasa, Yinchuan, and Beijing, due to the dominant clear sky. It can be further noted that the afternoon peak tends to be higher than the morning peak, which was also noted in Chen et al. (2018). However, locations with higher occurrence of overcast sky exhibit different PAR variation patterns. Wuhan and Changchun see the two peaks of the hourly PAR profile only in certain months. As the diffuse sky radiation constitutes a considerable portion of the total solar radiation, the double-peak pattern of PAR was hardly observed in Guangzhou and Chengdu.

The clear impact of seasons, climates and locations emphasizes the necessity of a climate-based dynamic analysis of PAR availability. The different response of the horizontal and vertical PAR availability to the greenhouse design, location and climate has demonstrated the superiority of predicting solar availability using a position-based method over the approaches in previous studies based on overall solar gain calculation.

5. Conclusions, design implications and future work

Based on simulation analysis, PAR availabilities in two large-scale greenhouses were studied in terms of five daylight climate zones, seven locations, and various orientations in China. Several conclusions and design implications are summarized as follows.

1) With the large-scale structure, the PAR availability at both horizontal and vertical planes has no clear link with roof configurations (A-frame or Barrel-vault). When planning an indoor farming facility like the greenhouse in China, the design of roofs could be determined by other issues such as cost and structure safety.

2) The impact of greenhouse orientation on PAR availability is found insignificant at the horizontal plane, while vertical planes see a high sensitivity of PAR availability to orientation. With an aim to improve productivities in Chinese greenhouses, the vertical arrangement of planting systems could be critical in terms of holistic greenhouse design and site planning.

3) The PAR availability in greenhouses is significantly affected by the combined conditions of location and climate in China. A climate-based analysis for the PAR availability would be necessarily required to achieve a practical and optimal greenhouse design and planning.

4) With the increasing requirement of vertical farming in greenhouses, it is necessary to predict solar availability (incl. PAR) using a position-based method instead of the previous models based on overall solar gain calculation. A ray-tracing solar modelling

(Radiance) could be very useful according to the accurate PAR prediction at a specific position.

Limitations and future work: This study has only investigated two typical greenhouse models with specific configurations and dimensions. No internal structures of greenhouse have been included in the simulation, which we believe would bring in some impacts on the solar transmittance through the envelop. The horizontal and vertical PAR availability was analysed based on an empty greenhouse without crops inside. The results could be different if the internal reflection from the plant is considered. In addition, surrounding structures that might shade the sun have not been considered. These issues will be addressed in further studies at the second stage.

Acknowledgement

The research of this paper was supported by the Shaanxi Provincial Key R&D Program - International Science and Technology Cooperation Program (2020KW-066).

References

Ahamed, M.S., Guo, H., Tanino, K., 2019. Energy saving techniques for reducing the heating cost of conventional greenhouses. Biosystems Engineering 178, 9–33. https://doi.org/10.1016/j.biosystemseng.2018.10.017

Alados, I., Foyo-Moreno, I., Alados-Arboledas, L., 1996. Photosynthetically active radiation: measurements and modelling. Agricultural and Forest Meteorology 78, 121–131. https://doi.org/10.1016/0168-1923(95)02245-7

Al-Helal, I.M., Waheeb, S.A., Ibrahim, A.A., Shady, M.R., Abdel-Ghany, A.M., 2015. Modified thermal model to predict the natural ventilation of greenhouses. Energy and Buildings 99, 1–8. https://doi.org/10.1016/j.enbuild.2015.04.013

Attar, I., Naili, N., Khalifa, N., Hazami, M., Lazaar, M., Farhat, A., 2014. Experimental study of an air conditioning system to control a greenhouse microclimate. Energy Conversion and Management 79, 543–553. https://doi.org/10.1016/j.enconman.2013.12.023

Bakirci, K., Ozyurt, O., Comakli, K., Comakli, O., 2011. Energy analysis of a solar-ground source heat pump system with vertical closed-loop for heating applications. Energy 36, 3224–3232.

https://doi.org/10.1016/j.energy.2011.03.011
Benli, H., 2013. A performance comparison between a horizontal source and a vertical source heat pump systems for a greenhouse heating in the mild climate Elaziğ, Turkey. Applied Thermal Engineering 50, 197–206. https://doi.org/10.1016/j.applthermaleng.2012.06.005
Benli, H., Durmuş, A., 2009. Performance analysis of a latent heat storage system with phase change material for new designed solar collectors in greenhouse heating. Solar Energy 83, 2109–2119. https://doi.org/10.1016/j.solener.2009.07.005
Benni, S., Tassinari, P., Bonora, F., Barbaresi, A., Torreggiani, D., 2016. Efficacy of greenhouse natural ventilation: Environmental monitoring and CFD simulations of a study case. Energy and Buildings 125, 276–286. https://doi.org/10.1016/j.enbuild.2016.05.014
Çakır, U., Şahin, E., 2015. Using solar greenhouses in cold climates and evaluating optimum type according to sizing, position and location: A case study. Computers and Electronics in Agriculture 117, 245–257. https://doi.org/10.1016/j.compag.2015.08.005
Campen, J.B., Bot, G.P.A., de Zwart, H.F., 2003. Dehumidification of Greenhouses at Northern Latitudes. Biosystems Engineering 86, 487–493. https://doi.org/10.1016/j.biosystemseng.2003.08.008
Cao, K., Xu, H., Zhang, R., Xu, D., Yan, L., Sun, Y., Xia, L., Zhao, J., Zou, Z., Bao, E., 2019. Renewable and sustainable strategies for improving the thermal environment of Chinese solar greenhouses. Energy and Buildings 202, 109414. https://doi.org/10.1016/j.enbuild.2019.109414
Chen, C., Li, Y., Li, N., Wei, S., Yang, F., Ling, H., Yu, N., Han, F., 2018. A computational model to determine the optimal orientation for solar greenhouses located at different latitudes in China. Solar Energy 165, 19–26. https://doi.org/10.1016/j.solener.2018.02.022
Chen, J., Ma, Y., Pang, Z., 2020. A mathematical model of global solar radiation to select the optimal shape and orientation of the greenhouses in southern China. Solar Energy 205, 380–389. https://doi.org/10.1016/j.solener.2020.05.055
Choab, N., Allouhi, A., El Maakoul, A., Kousksou, T., Saadeddine, S., Jamil, A., 2019. Review on greenhouse microclimate and application: Design parameters, thermal modeling and simulation, climate controlling technologies. Solar Energy 191, 109–137. https://doi.org/10.1016/j.solener.2019.08.042
Ciolkosz, D., 2008. Design daylight availability for greenhouses using supplementary lighting. Biosystems Engineering 100, 571–580. https://doi.org/10.1016/j.biosystemseng.2008.04.010
Cooper, P.I., Fuller, R.J., 1983. A transient model of the interaction between crop, environment and greenhouse structure for predicting crop yield and energy consumption. Journal of Agricultural Engineering Research 28, 401–417. https://doi.org/10.1016/0021-8634(83)90133-6
Cossu, M., Murgia, L., Ledda, L., Deligios, P.A., Sirigu, A., Chessa, F., Pazzona, A., 2014. Solar radiation distribution inside a greenhouse with south-oriented photovoltaic roofs and effects on crop productivity. Applied Energy 133, 89–100. https://doi.org/10.1016/j.apenergy.2014.07.070
Dong, T., Meng, J., Wu, B., Du, X., Niu, L., 2011. Overview on the Estimation of Photosynthetically Active Radiation. Progress in Geography 30, 1125–1134. https://doi.org/10.11820/dlkxjz.2011.09.007

Du, J., 2011. Assessing and predicting average daylight factors of adjoining spaces in atrium buildings under overcast sky. Building and Environment 11.

El-Maghlany, W.M., Teamah, M.A., Tanaka, H., 2015. Optimum design and orientation of the greenhouses for maximum capture of solar energy in North Tropical Region. Energy Conversion and Management 105, 1096–1104. https://doi.org/10.1016/j.enconman.2015.08.066

Fatnassi, H., Boulard, T., Lagier, J., 2004. Simple Indirect Estimation of Ventilation and Crop Transpiration Rates in a Greenhouse. Biosystems Engineering 88, 467–478. https://doi.org/10.1016/j.biosystemseng.2004.05.003

Ghoulem, M., El Moueddeb, K., Nehdi, E., Boukhanouf, R., Calautit, J.K., 2019. Greenhouse design and cooling technologies for sustainable food cultivation in hot climates: Review of current practice and future status. Biosystems Engineering 183, 121–150. https://doi.org/10.1016/j.biosystemseng.2019.04.016

Ghoulem, M., El Moueddeb, K., Nehdi, E., Zhong, F., Calautit, J., 2020a. Design of a Passive Downdraught Evaporative Cooling Windcatcher (PDEC-WC) System for Greenhouses in Hot Climates. Energies 13, 2934. https://doi.org/10.3390/en13112934

Ghoulem, M., El Moueddeb, K., Nehdi, E., Zhong, F., Calautit, J., 2020b. Analysis of passive downdraught evaporative cooling windcatcher for greenhouses in hot climatic conditions: Parametric study and impact of neighbouring structures. Biosystems Engineering 197, 105–121. https://doi.org/10.1016/j.biosystemseng.2020.06.016

Gorjian, S., Calise, F., Kant, K., Ahamed, M.S., Copertaro, B., Najafi, G., Zhang, X., Aghaei, M., Shamshiri, R.R., 2021. A review on opportunities for implementation of solar energy technologies in agricultural greenhouses. Journal of Cleaner Production 285, 124807. https://doi.org/10.1016/j.jclepro.2020.124807

Guo, Y., Zhao, H., Zhang, S., Wang, Y., Chow, D., 2020. Modeling and optimization of environment in agricultural greenhouses for improving cleaner and sustainable crop production. Journal of Cleaner Production 124843. https://doi.org/10.1016/j.jclepro.2020.124843

Gupta, M.J., Chandra, P., 2002. Effect of greenhouse design parameters on conservation of energy for greenhouse environmental control. Energy 27, 777–794. https://doi.org/10.1016/S0360-5442(02)00030-0

Gupta, R., Tiwari, G.N., Kumar, A., Gupta, Y., 2012. Calculation of total solar fraction for different orientation of greenhouse using 3D-shadow analysis in Auto-CAD. Energy and Buildings 47, 27–34. https://doi.org/10.1016/j.enbuild.2011.11.010

Hall, D.O., Rao, K., 1999. Photosynthesis. Cambridge University Press.

Hao, P.-F., Qiu, C.-W., Ding, G., Vincze, E., Zhang, G., Zhang, Y., Wu, F., 2020. Agriculture organic wastes fermentation CO2 enrichment in greenhouse and the fermentation residues improve growth, yield and fruit quality in tomato. Journal of Cleaner Production 275, 123885. https://doi.org/10.1016/j.jclepro.2020.123885

Harjunowibowo, D., Cuce, E., Omer, S.A., Riffat, S.B., 2016. Recent Passive Technologies of Greenhouse Systems-A Review. Presented at the 15th International Conference on Sustainable Energy Technologies – SET 2016, Singapore.

Iddio, E., Wang, L., Thomas, Y., McMorrow, G., Denzer, A., 2020. Energy efficient operation and modeling for greenhouses: A literature review. Renewable and Sustainable Energy Reviews

117, 109480. https://doi.org/10.1016/j.rser.2019.109480
IGDB (International Glazing Database) [WWW Document], 2019. . Lawrence Berkeley National Laboratory. URL https://windows.lbl.gov/software/igdb (accessed 11.10.19).
Ioslovich, I., Seginer, I., Gutman, P.-O., Borshchevsky, M., 1995. Sub-optimal CO2 Enrichment of Greenhouses. Journal of Agricultural Engineering Research 60, 117–136. https://doi.org/10.1006/jaer.1995.1006
Jain, D., Tiwari, G.N., 2002. Modeling and optimal design of evaporative cooling system in controlled environment greenhouse. Energy Conversion and Management 43, 2235–2250. https://doi.org/10.1016/S0196-8904(01)00151-0
Janjai, S., Wattan, R., Sripradit, A., 2015. Modeling the ratio of photosynthetically active radiation to broadband global solar radiation using ground and satellite-based data in the tropics. Advances in Space Research 56, 2356–2364. https://doi.org/10.1016/j.asr.2015.09.020
Kendirli, B., 2006. Structural analysis of greenhouses: A case study in Turkey. Building and Environment 41, 864–871. https://doi.org/10.1016/j.buildenv.2005.04.013
Kläring, H.-P., Hauschild, C., Heißner, A., Bar-Yosef, B., 2007. Model-based control of CO2 concentration in greenhouses at ambient levels increases cucumber yield. Agricultural and Forest Meteorology 143, 208–216. https://doi.org/10.1016/j.agrformet.2006.12.002
Kläring, H.-P., Klopotek, Y., Schmidt, U., Tantau, H.-J., 2012. Screening a cucumber crop during leaf area development reduces yield: Screening a cucumber crop. Ann Appl Biol 161, 161–168. https://doi.org/10.1111/j.1744-7348.2012.00560.x
Kooli, S., Bouadila, S., Lazaar, M., Farhat, A., 2015. The effect of nocturnal shutter on insulated greenhouse using a solar air heater with latent storage energy. Solar Energy 115, 217–228. https://doi.org/10.1016/j.solener.2015.02.041
Kozai, T., Niu, G., Takagaki, M., 2016. Plant Factory: An Indoor Vertical Farming System for Efficient Quality Food Production. Elsevier, London.
Kuroyanagi, T., Yasuba, K., Higashide, T., Iwasaki, Y., Takaichi, M., 2014. Efficiency of carbon dioxide enrichment in an unventilated greenhouse. Biosystems Engineering 119, 58–68. https://doi.org/10.1016/j.biosystemseng.2014.01.007
Lamnatou, Chr., Chemisana, D., 2013a. Solar radiation manipulations and their role in greenhouse claddings: Fresnel lenses, NIR- and UV-blocking materials. Renewable and Sustainable Energy Reviews 18, 271–287. https://doi.org/10.1016/j.rser.2012.09.041
Lamnatou, Chr., Chemisana, D., 2013b. Solar radiation manipulations and their role in greenhouse claddings: Fluorescent solar concentrators, photoselective and other materials. Renewable and Sustainable Energy Reviews 27, 175–190. https://doi.org/10.1016/j.rser.2013.06.052
Laouadi, A., 2005. Models of optical characteristics of barrel-vault skylights: development, validation and application. Lighting Research & Technology 37, 235–263. https://doi.org/10.1191/1365782805li141oa
Lee, S., Lee, I., Kim, R., 2018. Evaluation of wind-driven natural ventilation of single-span greenhouses built on reclaimed coastal land. Biosystems Engineering 171, 120–142. https://doi.org/10.1016/j.biosystemseng.2018.04.015
Li, A., Huang, L., Zhang, T., 2017. Field test and analysis of microclimate in naturally ventilated single-sloped greenhouses. Energy and Buildings 138, 479–489. https://doi.org/10.1016/j.enbuild.2016.12.047

Lu, M., Du, J., 2019. Dynamic evaluation of daylight availability in a highly-dense Chinese residential area with a cold climate. Energy and Buildings 193, 139–159. https://doi.org/10.1016/j.enbuild.2019.03.045

Mardaljevic, J., 1995. Validation of a lighting simulation program under real sky conditions. International Journal of Lighting Research and Technology 27, 181–188. https://doi.org/10.1177/14771535950270040701

McCartney, L., Orsat, V., Lefsrud, M.G., 2018. An experimental study of the cooling performance and airflow patterns in a model Natural Ventilation Augmented Cooling (NVAC) greenhouse. Biosystems Engineering 174, 173–189. https://doi.org/10.1016/j.biosystemseng.2018.07.005

Ministry of Agriculture and Rural Affairs of China, 2012. GB/T 29148-2012: Technical code for energy saving of greenhouses. Ministry of Agriculture and Rural Affairs of China, Beijing, China.

Ministry of Housing and Urban-Rural Development, 2013. Standard for Daylighting Design of Buildings. Beijing, China.

Mirzamohammadi, S., Jabarzadeh, A., Shahrabi, M.S., 2020. Long-term planning of supplying energy for greenhouses using renewable resources under uncertainty. Journal of Cleaner Production 264, 121611. https://doi.org/10.1016/j.jclepro.2020.121611

Mobtaker, H.G., Ajabshirchi, Y., Ranjbar, S.F., Matloobi, M., 2019. Simulation of thermal performance of solar greenhouse in north-west of Iran: An experimental validation. Renewable Energy 135, 88–97. https://doi.org/10.1016/j.renene.2018.10.003

Mobtaker, H.G., Ajabshirchi, Y., Ranjbar, S.F., Matloobi, M., 2016. Solar energy conservation in greenhouse: Thermal analysis and experimental validation. Renewable Energy 96, 509–519. https://doi.org/10.1016/j.renene.2016.04.079

Mortensen, L.M., 1986. Effect of relative humidity on growth and flowering of some greenhouse plants. Scientia Horticulturae 29, 301–307. https://doi.org/10.1016/0304-4238(86)90013-0

Neugebauer, M., Hałacz, J., Olkowski, T., 2021. A compost heating solution for a greenhouse in north-eastern Poland in fall. Journal of Cleaner Production 279, 123613. https://doi.org/10.1016/j.jclepro.2020.123613

Noorollahi, Y., Bigdelou, P., Pourfayaz, F., Yousefi, H., 2016. Numerical modeling and economic analysis of a ground source heat pump for supplying energy for a greenhouse in Alborz province, Iran. Journal of Cleaner Production 131, 145–154. https://doi.org/10.1016/j.jclepro.2016.05.059

Ntinas, G.K., Neumair, M., Tsadilas, C.D., Meyer, J., 2017. Carbon footprint and cumulative energy demand of greenhouse and open-field tomato cultivation systems under Southern and Central European climatic conditions. Journal of Cleaner Production 142, 3617–3626. https://doi.org/10.1016/j.jclepro.2016.10.106

Pakari, A., Ghani, S., 2019. Airflow assessment in a naturally ventilated greenhouse equipped with wind towers: numerical simulation and wind tunnel experiments. Energy and Buildings 199, 1–11. https://doi.org/10.1016/j.enbuild.2019.06.033

Panwar, N.L., Kaushik, S.C., Kothari, S., 2011. Solar greenhouse an option for renewable and sustainable farming. Renewable and Sustainable Energy Reviews 15, 3934–3945. https://doi.org/10.1016/j.rser.2011.07.030

Pearson, S., Wheldon, A.E., Hadley, P., 1995. Radiation Transmission and Fluorescence of Nine

Greenhouse Cladding Materials. Journal of Agricultural Engineering Research 62, 61–69. https://doi.org/10.1006/jaer.1995.1063
Perez, R., Pierre Ineichen, Robert Seals, Joseph Michalsky, Ronald Stewart, 1990. Modeling daylight availability and irradiance components from direct and global irradiance. Solar Energy 44, 271–289. https://doi.org/10.1016/0038-092X(90)90055-H
Perez, R., Seals, R., Michalsky, J., 1993. All-weather model for sky luminance distribution—Preliminary configuration and validation. Solar Energy 50, 235–245. https://doi.org/10.1016/0038-092X(93)90017-I
RADIANCE [WWW Document], 2020. URL www.radiance-online.org (accessed 7.10.20).
Reinhart, C.F., Walkenhorst, O., 2001. Validation of dynamic RADIANCE-based daylight simulations for a test office with external blinds. Energy and Buildings 33, 683–697. https://doi.org/10.1016/S0378-7788(01)00058-5
Sanjuan-Delmás, D., Llorach-Massana, P., Nadal, A., Ercilla-Montserrat, M., Muñoz, P., Montero, J.I., Josa, A., Gabarrell, X., Rieradevall, J., 2018. Environmental assessment of an integrated rooftop greenhouse for food production in cities. Journal of Cleaner Production 177, 326–337. https://doi.org/10.1016/j.jclepro.2017.12.147
Sethi, V.P., 2009. On the selection of shape and orientation of a greenhouse: Thermal modeling and experimental validation. Solar Energy 83, 21–38. https://doi.org/10.1016/j.solener.2008.05.018
Sharples, S., Lash, D., 2007. Daylight in Atrium Buildings: A Critical Review. Architectural Science Review 50, 301–312. https://doi.org/10.3763/asre.2007.5037
Singh, D., Basu, C., Meinhardt-Wollweber, M., Roth, B., 2015. LEDs for energy efficient greenhouse lighting. Renewable and Sustainable Energy Reviews 49, 139–147. https://doi.org/10.1016/j.rser.2015.04.117
Singh, R.D., Tiwari, G.N., 2010. Energy conservation in the greenhouse system: A steady state analysis. Energy, 7th International Conference on Sustainable Energy Technologies 35, 2367–2373. https://doi.org/10.1016/j.energy.2010.02.003
Stanciu, C., Stanciu, D., Dobrovicescu, A., 2016. Effect of Greenhouse Orientation with Respect to E-W Axis on its Required Heating and Cooling Loads. Energy Procedia, EENVIRO-YRC 2015 - Bucharest 85, 498–504. https://doi.org/10.1016/j.egypro.2015.12.234
Sun, Z., Liang, H., Liu, J., Shi, G., 2017. Estimation of photosynthetically active radiation using solar radiation in the UV–visible spectral band. Solar Energy 153, 611–622. https://doi.org/10.1016/j.solener.2017.06.007
Taki, M., Yildizhan, H., 2018. Evaluation the sustainable energy applications for fruit and vegetable productions processes; case study: Greenhouse cucumber production. Journal of Cleaner Production 199, 164–172. https://doi.org/10.1016/j.jclepro.2018.07.136
Teitel, M., Liran, O., Barak, M., Tanny, J., 2006. Air velocities in a naturally ventilated greenhouse. Acta Hortic. 189–196. https://doi.org/10.17660/ActaHortic.2006.719.19
Tong, G., Christopher, D.M., Li, T., Wang, T., 2013. Passive solar energy utilization: A review of cross-section building parameter selection for Chinese solar greenhouses. Renewable and Sustainable Energy Reviews 26, 540–548. https://doi.org/10.1016/j.rser.2013.06.026
Vadiee, A., Martin, V., 2014. Energy management strategies for commercial greenhouses. Applied Energy 114, 880–888. https://doi.org/10.1016/j.apenergy.2013.08.089

Vox, G., Teitel, M., Pardossi, A., Minuto, A., Tinivella, F., Schettini, E., 2010. Agriculture: technology, planning and management. In Sustainable Greenhouse Systems. Nova Science Publishers, Inc., New York, NY, USA.

Wang, Du, J., Li, D., 2019. A Simulation Study of Typical Green Houses in Beijing: PAR (Photosynthetically Active Radiation) Performances and Energy Consumption, in: Proceedings of the 16th IBPSA Conference. Presented at the Building Simulation 2019: 16th Conference of IBPSA, Rome, Italy, pp. 5006–5013. https://doi.org/10.26868/25222708.2019.210469

Zhang, S., Guo, Y., Zhao, H., Wang, Y., Chow, D., Fang, Y., 2020. Methodologies of control strategies for improving energy efficiency in agricultural greenhouses. Journal of Cleaner Production 274, 122695. https://doi.org/10.1016/j.jclepro.2020.122695

Zhou, Y., Xiang, Y., Shan, F., 2013. A climatological study on the photosynthetically active radiation. ACTA METEOROLOGICA SINICA 42, 387–397.